Carbonates and Evaporites (2022) 37:27
https://doi.org/10.1007/s13146-022-00770-9

ORIGINAL ARTICLE

Microfacies, physical and mechanical properties of carbonate rocks from the Apuseni Mountains, Romania: implication for delineating potential ornamental limestone extraction areas

Cristian Victor Mircescu[1] · Nicolae Har[1] · Tudor Tămaş[1]

Accepted: 3 April 2022 / Published online: 27 April 2022

Abstract

Ornamental rock quarrying and production represent an important segment of the raw material industry. This study aims to integrate key scientific concepts such as facies data, mineralogical analysis and physical–mechanical properties to delineate potential ornamental limestone extraction areas from the Apuseni Mountains, Romania. For this purpose, three distinct areas were evaluated, represented by the Moneasa, Subpiatră and Săndulești areas. The first two locations belong to the Northern Apuseni Mountains while the third location is situated in the Southern Apuseni Mountains. Eleven microfacies types were identified, consisting mainly of brecciated or nodular limestones, bioclastic packstones, boundstones, rudstones or silicified packstone. Microfacies types 4–8 and 9 are the most homogeneous in terms of colour and texture. Limestones with low porosity record higher uniaxial compressive strength values. This parameter is also influenced by porosity, micrite, sparite and grain proportion. The XRD analyses separate the samples in three major groups, based on their mineralogy. These include pure, detrital and silicified limestones. According to their strength, the studied limestones range from weak to tough and very tough rocks. Industrial-scale ornamental limestone quarrying was performed in the past only in the Moneasa Zone. These limestones were used especially for interior cladding and pavements. This study confirms their usage for such purposes. The Subpiatră Limestone is quarried extensively for cement production. However, this study shows that carbonate rocks from Subpiatră could be used for ornamental limestone production. Finally, the Săndulești Zone is analysed, in terms of ornamental stone potential. The physical and mechanical properties of these rocks suggests that these carbonate deposits are not suitable for ornamental rock quarrying.

Keywords Carbonates · Ornamental limestones · Microfacies · Physical properties · Mechanical properties

Introduction

Triassic—Upper Cretaceous carbonate rocks form extensive outcrops in various parts of the Apuseni Mountains (Ianovici et al. 1976). Ornamental limestone quarrying is an important industrial activity in various countries from the Mediterranean (Italy, Spain, Greece, Turkey, Croatia) (Calvo and Reguiero 2010), Portugal (Carvalho 1997; Carvalho et al. 2013; Carvalho and Lisboa 2018) and Germany (Siegiesmund et al. 2010). Limestones were used for this purpose since the antiquity and their aesthetic value is given by colour variations, structural and textural characteristics, mineralogy or physical and mechanical properties (Siegiesmund et al. 2010). All these properties are strongly influenced by the depositional environment and post-depositional processes such as tectonics and diagenesis (Murray and Pray 1965). Limestones, sandstones and marbles are quarried for ornamental purposes in various parts of Romania by numerous companies. These areas include Dobrogea, in SE Romania (sandstone—Başchioi) and the Poiana Ruscă Mountains, in SW Romania (marbles—Ruşchiţa). Ornamental limestones are exploited in the Apuseni Mountains from a wide range of deposits with ages ranging from Quaternary (Geoagiu-Băi, Cărpiniş, Hunedoara County)

✉ Cristian Victor Mircescu
cristian.mircescu@ubbcluj.ro

Nicolae Har
nicolae.har@ubbcluj.ro

Tudor Tămaș
tudor.tamas@ubbcluj.ro

1 Department of Geology, Babeş-Bolyai University, Mihail Kogălniceanu 1, 400084 Cluj-Napoca, Romania

to Miocene (Podeni, Cluj County) (Bucur et al. 2011) to Lower Jurassic (Moneasa, Arad County) (Tudoran 1997). This study presents a detailed description of carbonate rocks originating from deposits with different ages and lithologies (Lower Jurassic—Moneasa, Lower Cretaceous—Subpiatră, Badenian—Sândulești). Its main purpose is to highlight potential ornamental limestone exploitation areas by correlating microfacies characteristics with physical–mechanical properties and mineralogical composition. Ornamental limestones are defined as raw materials used for decorative purposes. Rocks can be exploited as ornamental material if their processing and quarrying does not affect in any way their internal structure (Carvalho and Lisboa 2018). The "*Ammonitico rosso"* facies characterises the Moneasa Limestone. Such red ammonite limestones were described for the first time in the mid-19th Century from Italy (Verona) (De Zigno 1850; Catullo 1853). Similar deposits form extensive outcrops in the Southern Alps, Western Carpathians (Misik 1964), Hungary (Pinter et al. 2014) and Western Greece (Robertson and Mountrakis 2006). This limestone was used extensively for the exterior cladding of some Romanian buildings (e.g. the House of Parliament and the House of Free Press in Bucharest and the Technical University of Cluj Napoca). Its petrographic, mineralogical and physical–mechanical properties are reassessed in this study since the Moneasa region was an active area until recent years (sensu Carvalho and Lisboa 2018). Badenian conglomerates from Sândulești were used by the Romans between the first and the third century AD for shaping blocks and architectural elements (Bărbulescu 1994). This study aims to decipher their ornamental stone potential by analysing their properties. Finally, a potential ornamental limestone exploitation perimeter is proposed for the Subpiatră area. These rocks are extensively quarried by LaFargeHolcim company for cement production.

Geological framework of the studied areas

Regional geology

The Moneasa and Subpiatră areas form an integrating part of the Northern Apuseni Mountains while the Sândulești area is located in the Southern Apuseni (Fig. 1). The Northern Apuseni consists of three major units: the Bihor Unit, the Codru Nappes (Lower and Upper) and the Biharia Nappes (Ianovici et al. 1976) (Fig. 1). The first two units contain an almost continuous Permo – Mesozoic carbonate and detrital succession (Fig. 1).

The Transylvanian nappes represent obduction nappes which form important outcrops in the Southern Apuseni Mountains and the internal Eastern Carpathians (Săndulescu et al. 1981; Balintoni 1997; Hoeck et al. 2009). Numerous previous studies were focussed on deciphering their tectonics (Lupu in Ianovici et al. 1976; Bleahu et al. 1981; Săndulescu 1984; Balintoni 1997; Schmid et al. 2008; Kounov and Schmid 2012). They comprise a calk-alkaline and a MORB-type ophiolite series with Upper Jurassic – Lower Cretaceous carbonate deposits (Fig. 1) (Kounov and Schmid 2012). Cretaceous flysch and wildflysch type deposits form their post-tectonic cover (Kounov and Schmid 2012) (Fig. 1).

Local geology

Moneasa zone

The Moneasa Zone is located in the Codru-Moma Massif (Fig. 1). The studied region belongs to the Finiș-Gârda Nappe from the Upper Codru Nappe System (Ianovici et al. 1976).

The Permian contains sandstones, diabases and porphyres (Fig. 2a) (Ianovici et al. 1976).

The Lower Triassic contains Werfenian sandstones and dolomites. The Middle Triassic deposits consist of Anisian – Ladinian carbonates (The Roșia limestone) and Ladinian limestones and detrital rocks (Fig. 2a) (Ianovici et al. 1976).

The Upper Triassic contains Carnian Dachstein Limestones and Carpathian Keuper type deposits (Fig. 2a) (Ianovici et al. 1976).

The Lower Jurassic consists of lower Sinemurian black-grey limestones that pass vertically into crinoidal grey-red limestones. They are covered by massive, nodular limestones with Gresten-type fauna, belemnites and brachiopods (upper Sinemurian – Pliensbachian) (Fig. 2a) (Ianovici et al. 1976).

The uppermost part of the Mesozoic succession contains Upper Jurassic – Berriasian flysch type deposits (Fig. 2a) (Ianovici et al. 1976).

The studied deposits belong to the Lower Jurassic (lower Sinemurian – Pliensbachian) succession of the Moneasa Zone.

Subpiatră zone

This area is an integrating part of the Bihor Unit which forms extensive outcrops throughout the Northern Apuseni Mountains (Patrulius in Ianovici et al. 1976). The sedimentary unit consists of Permian – Turonian deposits that cover the metamorphic basement of the Someș Series (Patrulius in Ianovici et al. 1976).

Middle Jurassic – Lower Cretaceous rocks form the bulk of the sedimentary succession from the Subpiatră Zone (Fig. 2b).

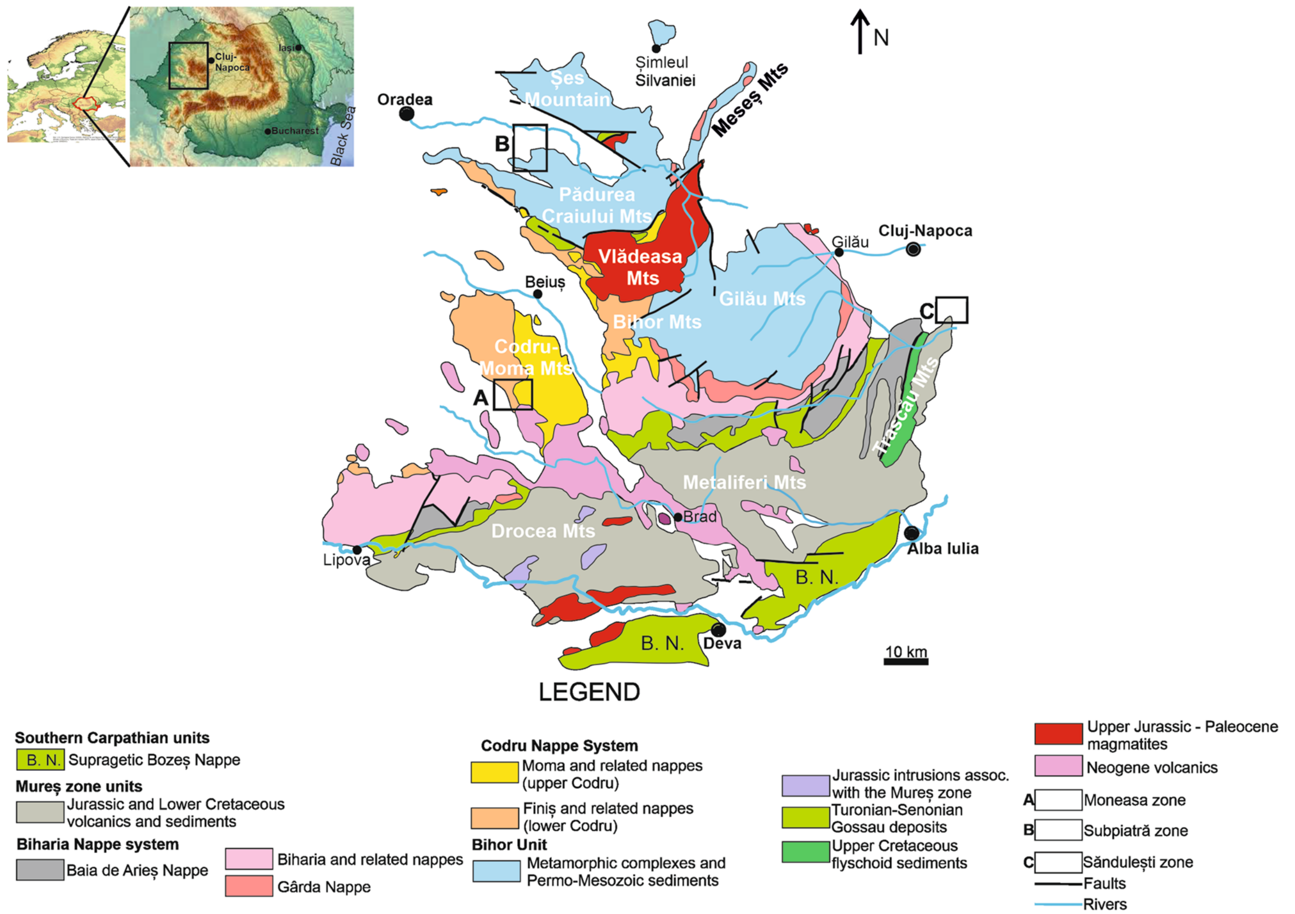

Fig. 1 Location of the most important tectonic units from the Northern and Southern Apuseni Mountains. **a**—Moneasa Zone; **b**—Subpiatră Zone; **c**—Sândulești Zone (modified from Bleahu et al. 1981; Săndulescu 1984; Balintoni and Puște 2002; Balintoni et al. 2009)

The Middle Jurassic contains mainly marls, ooidic and glauconitic limestones (Patrulius in Ianovici et al. 1976) (Fig. 2b).

The Upper Jurassic deposits consist of reefal and inner platform carbonates and they are divided in four major lithostratigraphic units, namely the Vad, Cornet, Aștileu and Albioara formations (Cociuba 2000) (Fig. 2b).

Subsequently, the Lower Cretaceous succession is divided by Patrulius (in Ianovici et al. 1976) in the following units (Fig. 2b): (1) Bauxites; (2) Black limestones with charaeans; 3) Micritic limestones with gastropods; (4) Lower Pachiodont limestones; (5) Ecleja Marls; (6) Middle Pachiodont limestones; (7) Glauconitic sandstones and Upper Pachiodont Limestones.

According to recent studies (Cociuba 2000; Bucur 2000 and Bucur et al. 2010), the Lower Cretaceous succession from this area includes the following lithostratigraphic units: (1) The Blid Formation (Berriasian-Barremian); (2) The Ecleja Formation (lower Aptian); (3) The Valea Măgurii Formation (lower Aptian); (4) The Vârciorog Formation (upper Aptian – Albian).

The studied deposits belong to the Subpiatră Limestone which is an integrating part of the upper Aptian – Albian Vârciorog Formation (Bucur et al. 2010).

Sândulești zone

The sedimentary succession from the Sândulești Zone contains Upper Jurassic limestones disposed over Jurassic island arc type igneous rocks (Fig. 3). These carbonate rocks contain alternances of hemipelagic limestones and grainflows associated with bioconstructions and coarse reef debris (Săsăran 2006). The entire Mesozoic succession is covered by Badenian carbonate conglomerates and microconglomerates (Fig. 3). They represent the lowermost part of the Cenozoic succession from the Western part of the Transylvanian Basin (Filipescu and Gârbacea 1997).

The studied deposits consist of Badenian carbonate microconglomerates with Upper Jurassic limestone elements.

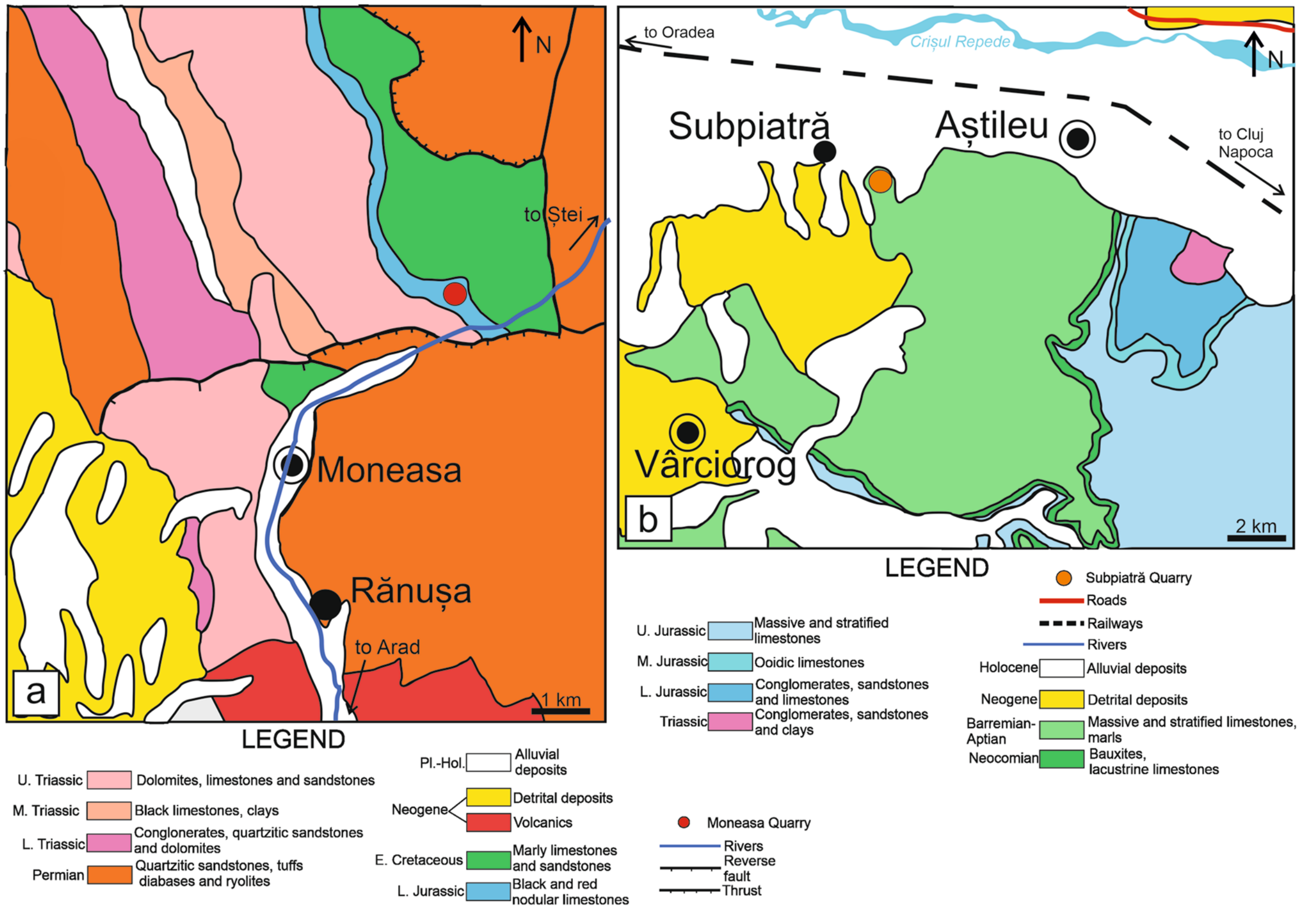

Fig. 2 Location of the Moneasa and Subpiatră quarries (**a**—geological structure of the Moneasa Zone and the exact location of the Moneasa quarry within the Lower Jurassic succession of the area; **b**—geological structure of the Subpiatră Zone and the location of the Subpiatră quarry within the Mesozoic succession of the studied area) (modified from Bleahu et al. 1967 and Giușcă et al. 1968)

Methodology

Fieldwork campaigns

A total number of 30 samples were collected during several fieldwork campaigns. Sampling was performed by collecting at least one representative sample from each carbonate rock bank. Sixteen samples were collected for thin section preparation and 14 samples were used for physical mechanical analysis.

Thin section and polished slab analysis

Polished slabs were prepared and high-resolution image scanning (resolution of 1200 dpi) was performed to highlight colour changes and the presence of fractures and other heterogeneities, then the most important surfaces were delineated and twenty thin sections were prepared.

Carbonate microfacies description follows Dunham (1962). Additional descriptions were performed by following the classification scheme of Siegiesmund et al. (2010). According to this author, carbonate rocks consist of major constituents, pores, fractures and stylolites.

X-ray diffraction analysis

Thirteen selected carbonate rock samples were analysed by X-ray diffraction (XRD) to evaluate their mineralogical composition. Five grams of representative samples were milled in an agate mortar, were subsequently quartered and then analysed with a Bruker D8 Advance diffractometer with a CuKα tube ($\lambda = 1.5418$ Å) operating at 40 kV/40 mA, a Ni 0.0125 mm filter and a LynxEye detector. Diffraction patterns were collected between 5° and 64° 2θ with a step of 0.02° and a counting time of 0.2 s/step. The DiffracEVA (2.1 ver.) program with the PDF2 database from ICDD (International Center for Diffraction Data) were used for mineral identification.

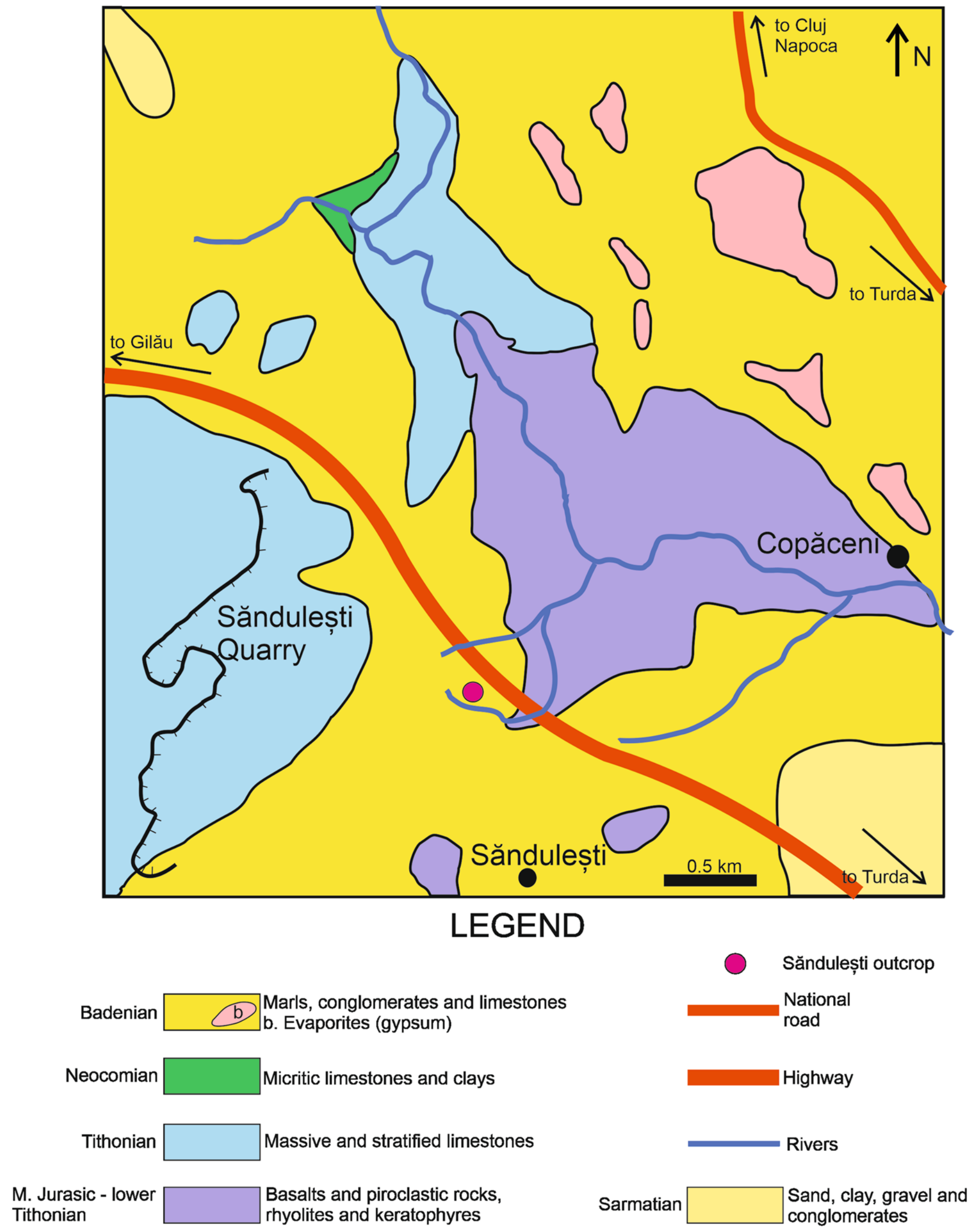

Fig. 3 Location of the Săndulești outcrop and the geological structure of the Săndulești–Tureni Zone (modified from Rusu et al. 2018)

Apparent density, mineral skeleton density, porosity

These physical–mechanical properties were determined by applying the Romanian Standard STAS 6200/13-80 (1974). Equivalent analysis methods can be found in the SR EN 1097-6:2002 standard.

One method was used for the apparent density measurements.

It involved apparent volume measurement with the hydrostatic balance on dry, paraffin covered samples. Subsequently, the apparent density was expressed as the ratio between the mass of the dry sample and the apparent volume.

The apparent volume has the following formula:

$$V_a = \left[(m_1 - m_2)/\rho_w\right] - \left[(m_1 - m)/\rho_p\right],$$

where V_a is the apparent volume (in cm^3), m_1 is the paraffin covered sample mass, determined with the hydrostatic balance in the air (in grams), m_2 is the paraffin covered sample mass, determined with the hydrostatic balance in the water (in grams), m is the dry sample mass (in g), ρ_w is the water density (in g/cm^3) ($\rho_w = 1$ g/cm^3) and ρ_p is the paraffin density (in g/cm^3) ($\rho_p = 0.92$ g/cm^3).

Mineral skeleton density was determined by applying pycnometry methods according to the Romanian Standard

STAS 6200/13-80 (1974) and the SR EN 1097-6:2002 standard. The following formula was used:

$$\rho_s = m_1/\left(m_1 + m_2 - m_3\right),$$

where m_1 is the dry sample mass (in g), m_2 is the water-filled pycnometer mass, and m_3 is the water and powder-filled pycnometer mass.

Total porosity has the following formula: $n_t(\%) = \left[1-\left(\rho_a/\rho_s\right)\right] \times 100$, where ρ_a is the apparent density (in g/cm^3) and ρ_s is the density of the mineral skeleton (in g/cm^3).

Uniaxial compressive strength

A total number of 26 cube shaped specimens, with 50 mm edges were prepared, from 14 samples collected from the field. Where possible, the uniaxial compression was applied on planar surfaces which are perpendicularly on fissures or fractures. The uniaxial compressive strength was expressed as the ratio between the force and the surface on which compression is performed.

Thin-section preparation, XRD analysis and physico-mechanical measurements (porosity, density and uniaxial compressive strength) were performed at Babeş-Bolyai University from Cluj Napoca.

Results

All the studied samples can be grouped in 10 lithofacies and 11 microfacies types, while the physical and mechanical properties record important variations. The apparent density ranges between 2.48 and 2.72 g/cm^3, the mineral skeleton density has a minimum value of 2.60 g/cm^3 and a maximum of 2.75 g/cm^3 and the uniaxial compressive strength ranges between 756 MPa and 144,81 MPa. The XRD analysis indicates the presence of three major groups based on sample mineralogy.

Outcrop description

Moneasa zone

The studied outcrop is located in the Moneasa-Băi Quarry from the Piatra cu Lapte Hill. The entire outcrop consists of 15 limestone banks. Samples were taken from banks 1–2 and 4–8. Their individual thickness decreases from base to top (Fig. 4a, b, f). The first three banks consist of 3- to 5 m-thick black limestones with calcite filled voids and fractures (Fig. 4a). Repetitive facies characterise the middle part of the quarry (Fig. 4c–e): the first carbonate bank contains reddish, compact limestones, cross-cut by vertical to oblique calcite veins, delimited by brecciated, nodular facies types at the base and the top. The brecciation structures contain a mixture of clay material and iron oxides (Fig. 4d, e).

Subpiatră zone

The studied outcrops are located in the Subpiatră Quarry, property of LaFarge Holcim company. The first sector is situated in the western part of the quarry, approximately 2 km east from Subpiatră locality (Fig. 5a, b). Decimetre–metre-thick grey limestone banks characterise this area (Fig. 5c). They contain rudists, corals, microbial and *Bacinella* type structures (Fig. 5c, d). The second sector is located in the upper part of the quarry (Fig. 6a). The limestones contain rudists and *Bacinella* type structures (Fig. 6b, c).

Săndulești zone

The studied outcrops are located approximately 200 m south-west of the Gilău-Câmpia Turzii Highway, near the Roman Spring, in the vicinity of the Săndulești Limestone Quarry (Fig. 7a, b, d). Two main units of carbonate–siliciclastic rocks characterise this zone. Unit A corresponds to a 7 m-thick bank while unit B consists of 3 m thick, thinning upward, superimposed beds (Fig. 7e, f). Decimetre–metre-scale pebbles and cobbles are present (Fig. 7c).

Polished slab analysis

Moneasa zone

The polished slab analysis of this zone indicates the presence of four major facies types:

Lithofacies 1—homogeneous, black, fine to medium packstone which lacks fissures or fractures (Fig. 8a).

Lithofacies 2—red, crinoidal wackestone–packstone with calcite filled voids (Fig. 8c).

Lithofacies 3—dark red wackestone with calcite-filled fissures (Fig. 9a, e) and voids (Fig. 8g).

Lithofacies 4—nodular, brecciated wackestone. Clay material and iron oxides are present between the carbonate nodules (Figs. 8e, 9c, g).

Subpiatră zone

Three main lithofacies types were identified by analysing the polished slabs from this area:

Lithofacies 5—wackestone–packstone with bivalves (Fig. 6g) and *Bacinella* type structures (Fig. 10d). Millimetre-to-centimetre-thick nodules are present, surrounded by submillimetre-thick coatings (Fig. 10d). Fractures are missing and porosity is absent. The carbonate sediment contains encrusting organisms and worm tubes.

Fig. 4 Detailed outcrop images from the Moneasa Quarry [**a**—carbonate banks from the lowermost part of the quarry (black lines). Their thickness ranges between 3 and 5 m. Note the presence of sparite filled voids and fissures; **b**—general view of the quarry. Bed thickness decreases form base to top. The black rectangle indicates the exact position of **c**. The white rectangle indicates the position of **d** while the yellow rectangle indicates the position of **f**; **c**—carbonate unit from the middle part of the quarry. It contains brecciated and nodular red limestones; **d**, **e**—alternances of brecciated, nodular and crinoidal red limestones. The non-brecciated areas are cross-cut by a system of fissures which are parallel with the bedding planes. In addition, they are intercepted by vertical cracks that contain sparite. The black rectangle in **d** indicates the exact position of **e**; **f**—thinning upward beds from the uppermost part of the quarry) (scale: **a**, **f**—2 m; **b**, **d**—1 m; **c**—20 cm; **e**—40 cm)

Fig. 5 Detailed outcrop images from the Subpiatră Quarry (**a**—location of the Subpiatră Quarry at the northern edge of a calcareous massif consisting mainly of the Upper Aptian – Albian Subpiatră limestone; **b**—sampling direction across decimetre–metre-thick carbonate beds (white arrow). The exact position of the abandoned quarry sector is indicated by the black rectangle and the down-left corner detailed image; **c**—decimetre–metre-thick carbonate beds; **d**—detailed view of a rudist bearing metre-thick carbonate bed)

Lithofacies 6—Coarse bioclastic grainstone–rudstone with rudist fragments. The rock contains bivalves and other bioclasts (Fig. 10a).

Lithofacies 7—Rudist boundstone (Fig. 10f) with bioclastic packstone–grainstone internal sediment. It contains gastropods, bivalves and dasycladalean algae. The rock lacks any fractures or fissures and it has a grey colour. Darker areas are associated with *Bacinella* type structures.

Sănduleşti zone

The following lithofacies were identified in polished slabs:

Lithofacies 8—yellowish light grey wackestone–packstone with rare microfossils (Fig. 11a).

Lithofacies 9—dark grey bioclastic intraclastic rudstone with subangular intraclasts (Fig. 11c).

Lithofacies 10—carbonate microconglomerate-sandstone with quartz fragments and grey micritic intraclasts (Fig. 11e, g).

Petrographic and microfacies analysis

Moneasa zone

Microfacies type 1 (Samples 2445 b–2446)—bioclastic packstone (Fig. 12). Bioclasts are represented by foraminifera, echinoderm plates and bivalves (Fig. 8b). Intraclasts and fractures are absent (Fig. 8b). The stylolites are filled with dark, black material.

Microfacies type 2 (Samples 2448 a, 2452 b)—stylolised crinoidal wackestone–packstone (Figs. 8d, 12). This lithofacies type contains abundant echinoderm plates (Fig. 8d), thin shell bivalves (Fig. 8d), foraminifera and sponge spicules. Intraclasts are absent and syntaxial over-growth cement is developed around the echinoderm plates (Fig. 8d). The stylolites contain clay material and iron oxides and they commonly develop between echinoderm plates or other bioclasts (Fig. 8d). Interparticle porosity is lost by cementation (Fig. 8d).

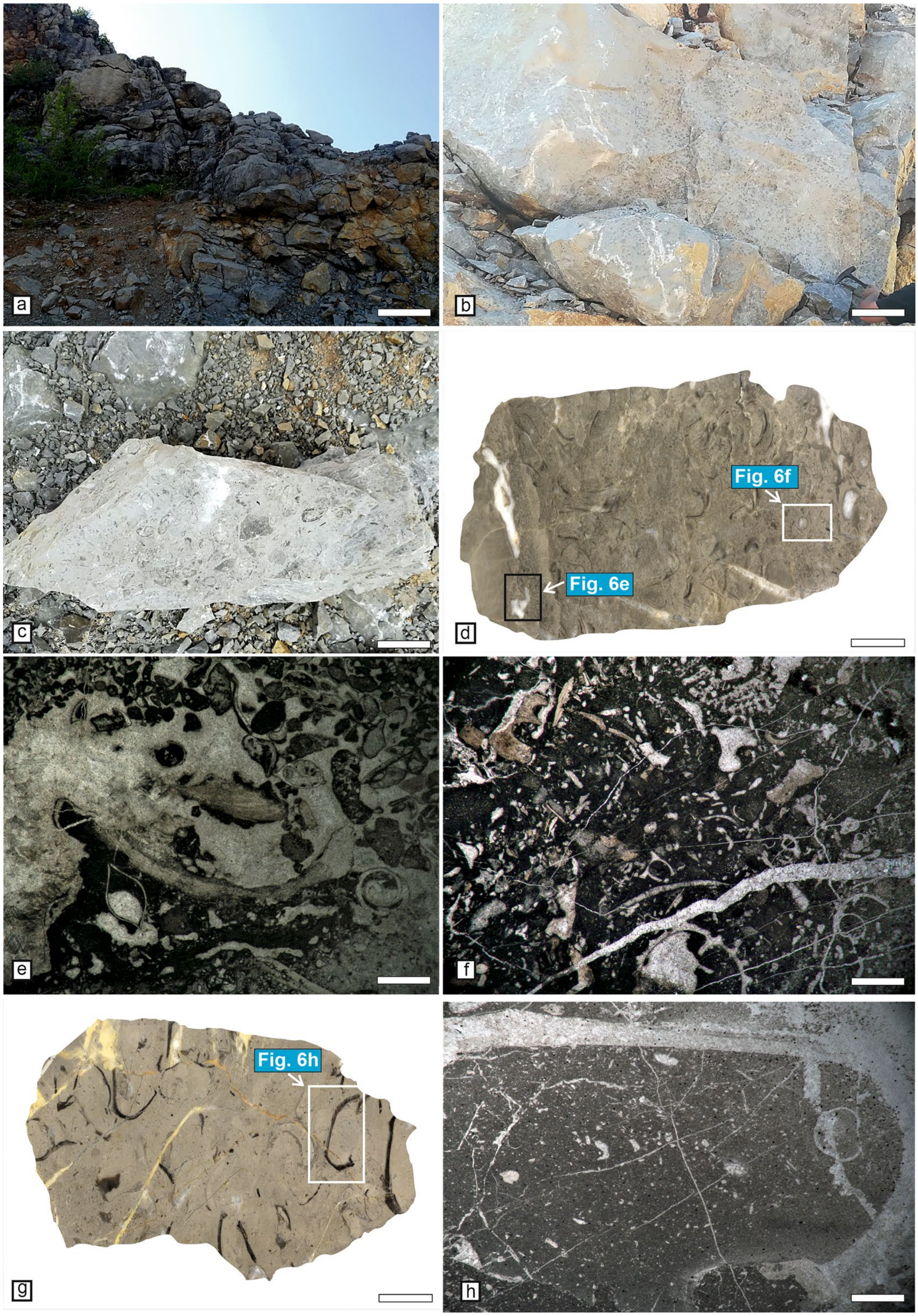

Fig. 6 Outcrop, polished slab and thin section images from the northern part of the Subpiatră Quarry (**a**—strongly fissured carbonate rocks; **b**—wackestone with *Bacinella* type structures; **c**—bioclastic grainstone–rudstone with rudist fragments; **d**—polished slab indicating a gradual transition from a boundstone to a bioclastic rudstone and packstone–grainstone. The black rectangle indicates the position of the microphotograph from **e** while the white rectangle indicates the exact position of the microphotograph from **f**; **e**—former growth-framework, cavity and shelter porosity. All the porosities are lost by cementation; **f**—bioclastic packstone with gastropods, cyanobacteria nodules and dasycladalean algae; **g**—polished slab through a bioclastic wackestone with bivalves. The white rectangle indicates the exact position of the microphotograph from **h**; **h**—wackestone with bivalves and gastropods) (scale: **a**—1 m; **b**, **c**—10 cm; **d**, **g**—2 cm; **e**, **f**, h—2 mm)

Fig. 7 Outcrop images from the Săndulești area (**a**—Badenian carbonate microconglomerates surrounding the Roman Spring; **b**—Badenian carbonate microconglomerates with thinning upward tabular beds. The white rectangle indicates the position of **c**; **c**—decimetre–metre-thick Upper Jurassic pebbles and cobbles encased in younger Badenian deposits; **d**—general view of the Săndulești outcrop; **e**, **f**—thinning upward beds of Badenian carbonate microconglomerates. The entire outcrop consists of two units: A and B (white letters). Vertical fractures cross-cut these units) (scale: **a**, **c**, **d**—1 m; **b**, **f**—2 m; **e**—3 m)

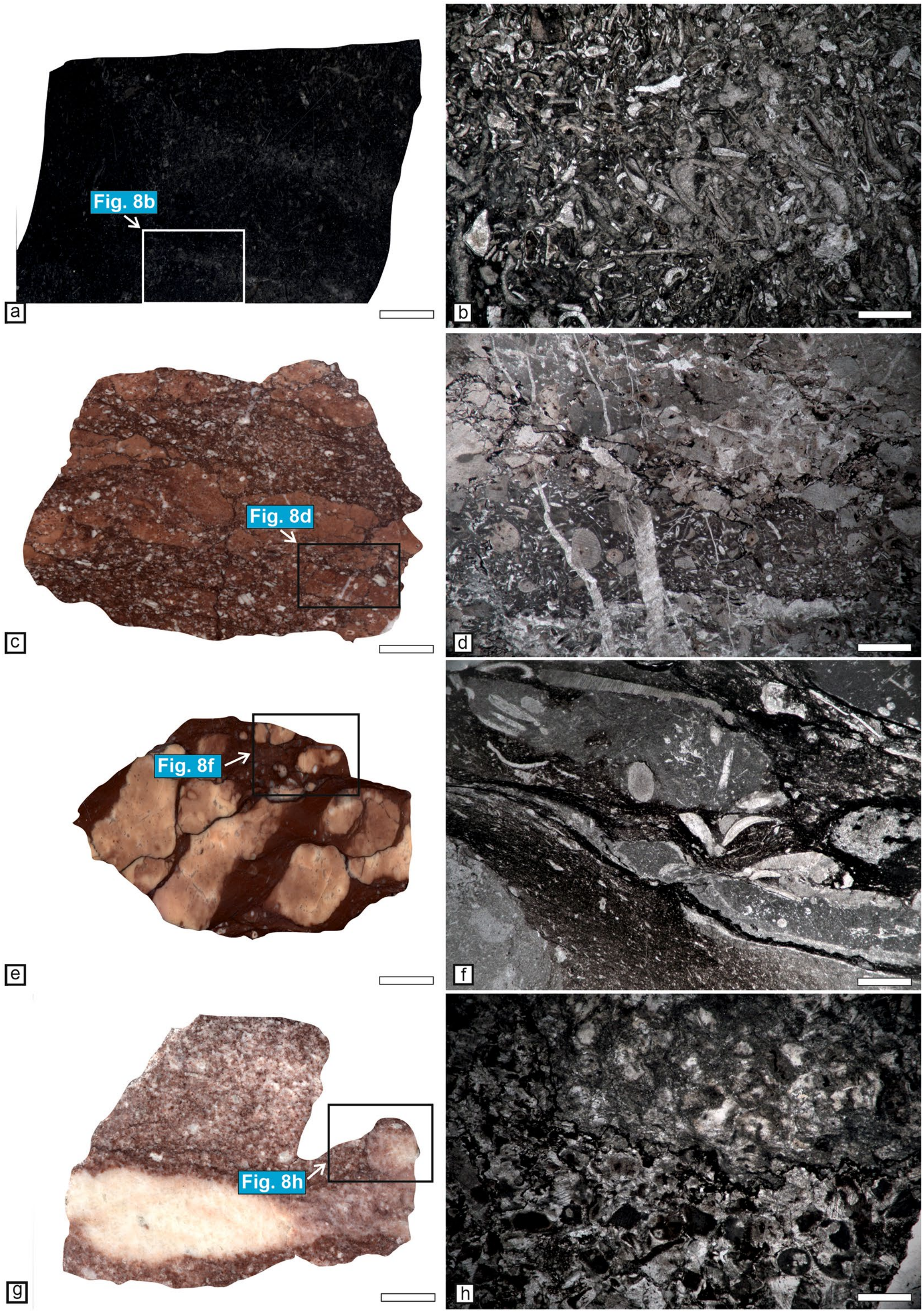

Fig. 8 Polished slabs and thin-section images from the Lower Jurassic limestones of the Moneasa Quarry (**a**—black homogeneous packstone. The white rectangle indicates the position of the microphotograph from **b**; **b**—bioclastic packstone with abundant bivalves and foraminifera. Intraclasts and fractures are missing; **c**, **d**—crinoidal, stylolite rich wackestone–packstone. It contains echinoderm plates, thin shell bivalves. Stylolites cross-cut the sparitic overgrowth cement which is developed around the echinoderm plates. The black rectangle in **c** indicates the exact position of **d**; **e**, **f**—brecciated nodular wackestone. The areas between the carbonate nodules contain interlayered, thin levels of iron oxides and detrital material. Bioclasts consist of thin shell bivalves and echinoderms. The black rectangle in **e** indicates the exact position of **f**; **g**, **h**—silicified crinoidal packstone. Rare stylolites are filled with iron oxides. The black rectangle in **g** indicates the exact position of **h**) (scale: **a**, **c**, **e**, **g**—2 cm; **b**, **d**, **f**, **h**—2 mm)

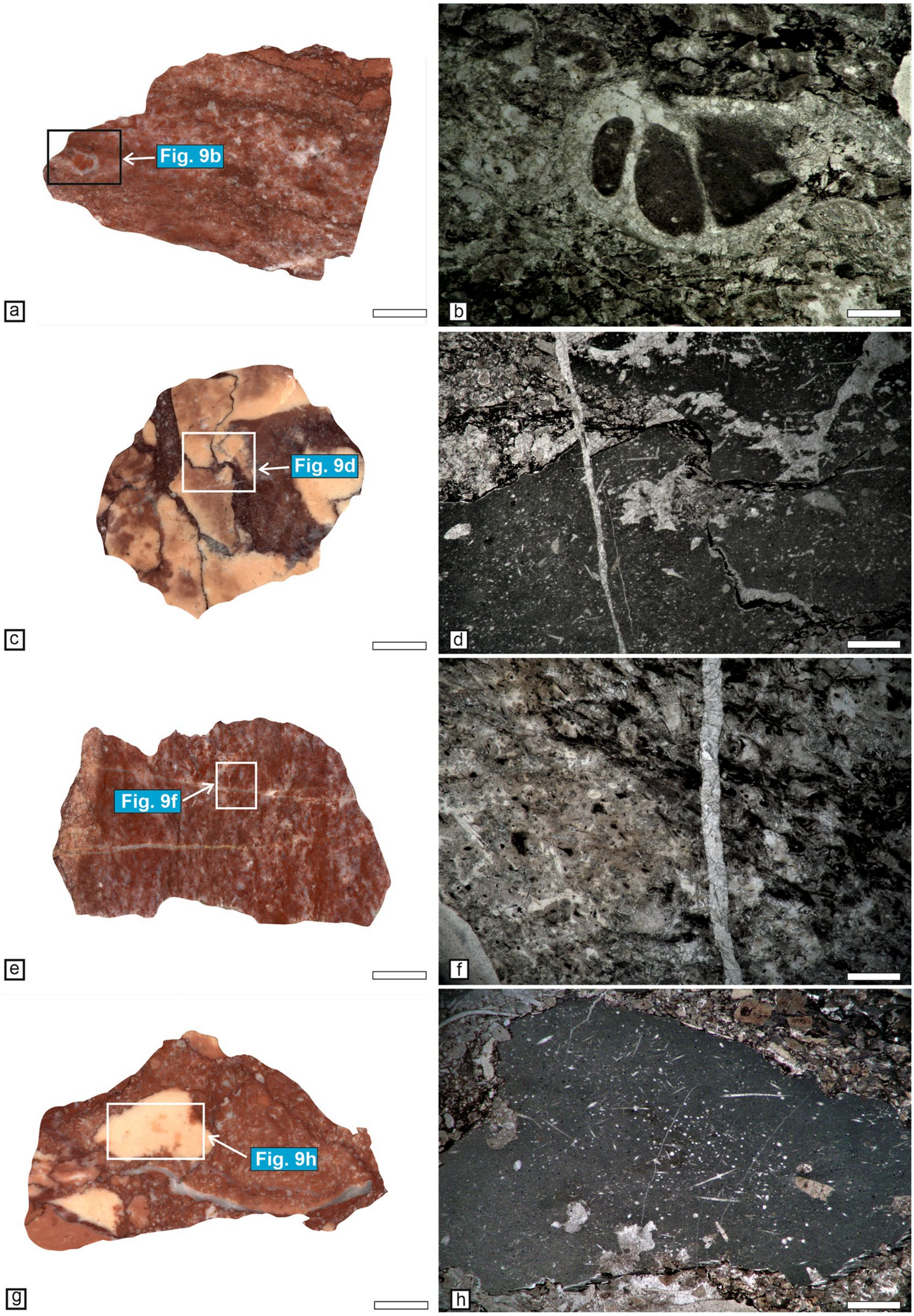

Fig. 9 Polished slabs and thin section images from the Lower Jurassic limestones of the Moneasa Quarry (**a**, **b**—silicified crinoidal packstone containing gastropods and rare foraminifera. The black rectangle in **a** indicates the exact position of the thin-section microphotograph from **b**; **c**, **d**—nodular brecciated wackestone–packstone. It contains thin shell bivalves and sponge spicules. The white rectangle from **c** indicates the exact position of **d**; **e**, **f**—silicified crinoidal packstone. The white rectangle in **e** indicates the exact position of the microphotograph from **f**; **g**, **h**—brecciated nodular limestone. It contains two facies types: pelagic wackestone with echinoderm plates and sponge spicules and crinoidal packstone. Rare stylolites are present between the echinoderm plates. The white rectangle in **g** indicates the exact position of the microphotograph from **h**) (scale: **a**, **c**, **e**, **g**—2 cm; **b**, **d**, **f**, **h**—2 mm)

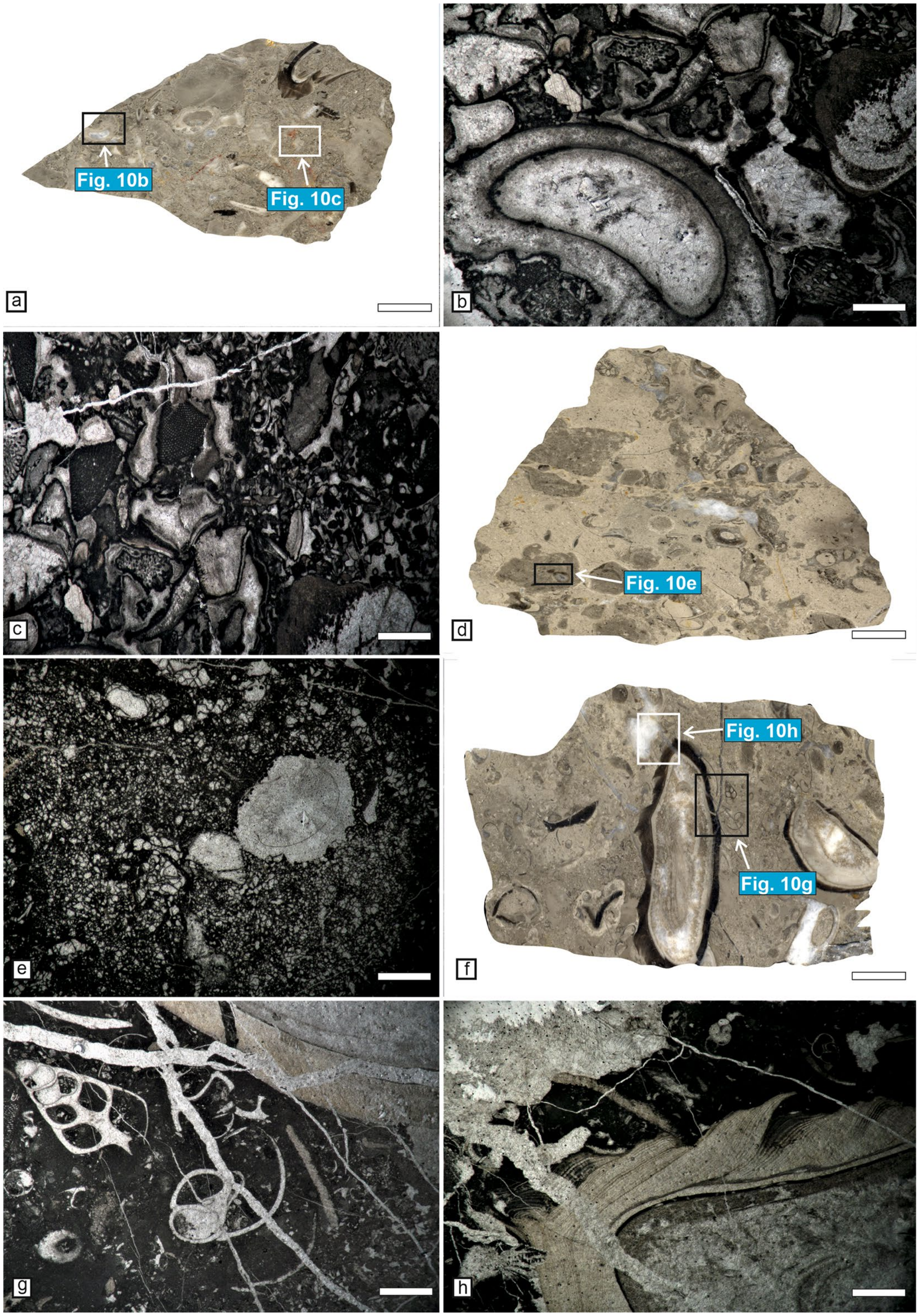

Fig. 10 Polished slabs and thin sections from the Upper Aptian–Albian limestones of the Subpiatră quarry (**a**—polished slab through a bioclastic rudstone. The black rectangle indicates the exact position of the microphotograph from **b** while the white rectangle indicates the position of the microphotograph from **c**; **b**, **c**—bioclastic grainstone–rudstone with gastropods, coral fragments, dasycladalean algae and orbitolinid type foraminifera; **d**—wackestone with *Bacinella* type structures. There is a colour difference between the bioclasts and the matrix. The matrix is light grey while the bioclasts have a dark grey colour. The black rectangle indicates the exact position of the microphotograph from **e**; **e**—detailed microphotograph of a nodule composed of *Bacinella* type structures; **f**—polished slab through a rudist bearing boundstone. Pores are completely filled by calcite. The white and black rectangles indicate the position of the microphotographs from **g**, **h**; **g**, **h**—packstone type internal sediment with gastropods and thin shell bivalves) (scale: **a**, **d**, **f**—2 cm; **b**, **c**, **e**, **g**, **h**—2 mm)

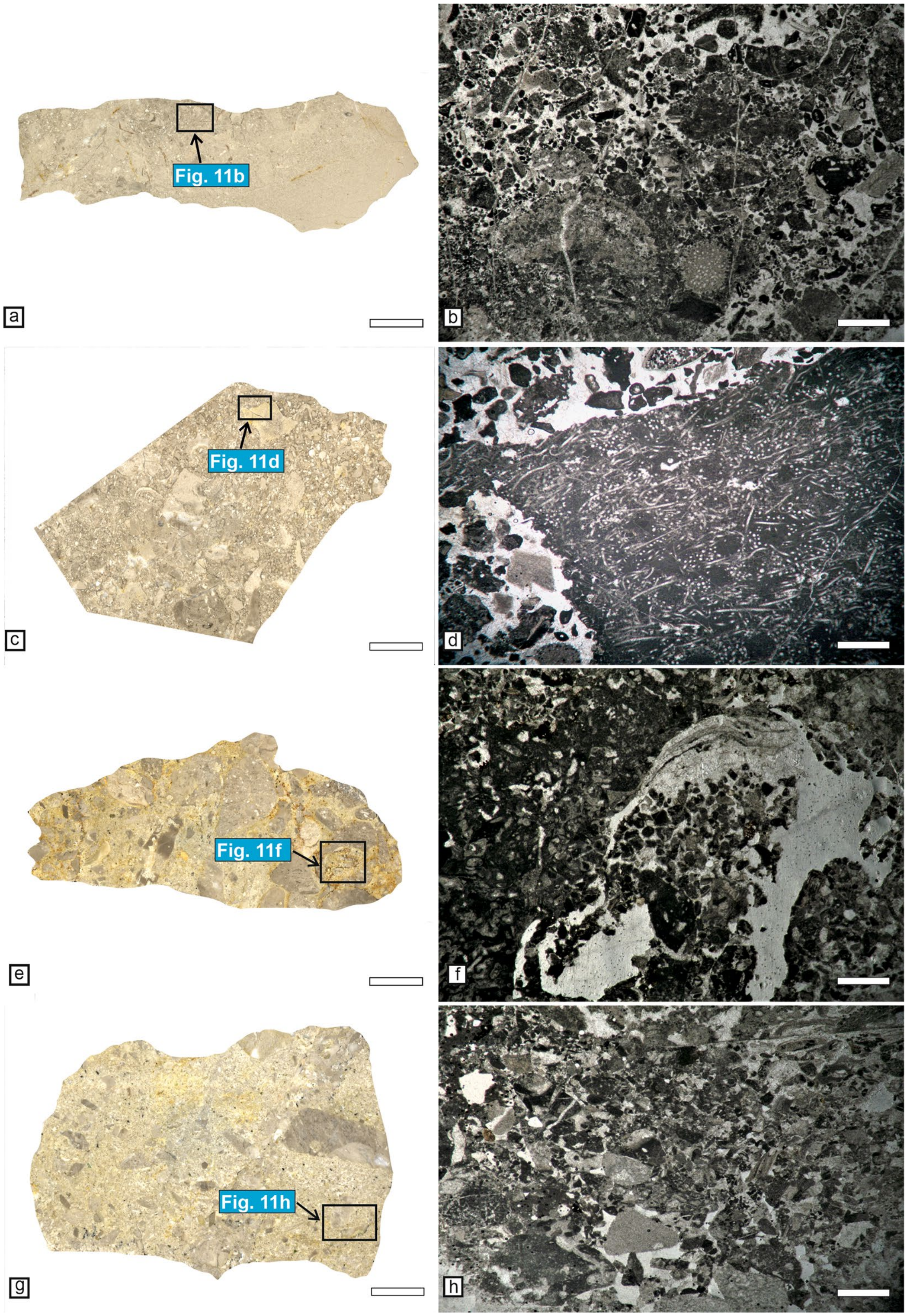

Microfacies type 3 (Samples 2448 b, 2450)—brecciated nodular wackestone (Figs. 8f, 12). Bioclasts are represented by thin shell bivalves, sponge spicules and echinoderm plates. Millimetre-thick laminae develop between the carbonate nodules. This filling consists of superimposed layers of clay material and iron oxides (Fig. 8f). It may contain rare bioclasts.

Microfacies type 4 (Samples 2449, 2451, 2453)—this microfacies type consists of crinoidal silicified packstone (Figs. 8h, 9b, f, 12).

◂**Fig. 11** Polished slabs and thin sections from the Upper Jurassic and Badenian carbonate deposits of Săndulești (**a**—polished slab indicating a transition from a bioclastic grainstone to peloidal wackestone. The black rectangle indicates the exact position of the microphotograph from **b**; **b**—bioclastic grainstone with encrusting organisms and calcareous sponges; **c**—polished slab through a bioclastic rudstone. The black rectangle indicates the exact position of the microphotograph from **d**; **d**—bioclastic intraclastic rudstone with echinoderm plates and large calcareous sponges; **e**, **g**—polished slabs through carbonate microconglomerates. They contain centimetre scale carbonate pebbles originating from Upper Jurassic reefal deposits. The black rectangles indicate the exact position of the microphotographs from **f**, **h**; **f**—Vug-type porosity affecting the matrix of a carbonate microconglomerate; **h**—carbonate microconglomerate matrix with echinoderm plates and quartz fragments. Interparticle porosity is developed between echinoderm plates and peloids) (scale: **a**, **c**, **e**, **g**—2 cm; **b**, **d**, **f**, **h**—2 mm)

Microfacies type 5 (Sample 2452 a)—brecciated and stylolised wackestone–packstone (Figs. 9d, 12) with sponge spicules, echinoderm plates and thin shell bivalves. The brecciated zones contain sparite, bioclasts, iron oxides and clay material (Fig. 9d).

Microfacies type 6 (Samples 2454 a–b)—nodular, brecciated limestone, consisting of two subfacies types: pelagic wackestone with echinoderm plates and sponge spicules and crinoidal packstone (Fig. 9h). The stylolites develop between bioclasts (echinoderm plates), on areas with overgrowth cement (Fig. 9h).

Subpiatră zone

Microfacies type 7 (Samples 2455, 2466, 2467, 2472)—boundstone with bioclastic packstone–grainstone internal sediment (Figs. 6e, f, 10f–h, 12). It contains corals, gastropods, bivalves, dasycladalean algae, cyanobacteria nodules, foraminifera, *Bacinella* type structures and rudist fragments (Fig. 6e, f). Corals are perforated through bioerosion and the resulting voids are filled with micrite. Rounded to well-rounded peloids are common and their average dimension has 30 microns. Growth-framework porosity is lost by cementation (Fig. 6d, e).

Microfacies type 8 (Samples 2456, 2457, 2466, 2467)—bioclastic rudstone (Fig. 12). Microfossils are represented by gastropods, orbitolinids, dasycladalean algae, rudists and coral fragments (Fig. 10b, c). Peloids are present and their dimension ranges from 10 to 20 microns. Intraparticle and vuggy type pores are completely filled with granular cement (Fig. 10a). The sample contains terrigenous material.

Microfacies type 9 (Samples 2458, 2465, 2455, 2468, 2469, 2471)—wackestone–floatstone (Fig. 12) with thick shell bivalves (Fig. 6g, h), rudists and *Bacinella* type structures. Microfossils are represented by foraminifera, bivalves, echinoderms, gastropods, large dasycladalean algae, rudists and *Bacinella* nodules (Fig. 10d, e).

Săndulești zone

Microfacies type 10 (Samples 2438–2440)—coarse bioclastic grainstone–rudstone (Figs. 11a-d, 13). The rocks contain encrusting organisms [*Crescentiella morronensis* (Crescenti) (Fig. 11b, d), *Lithocodium aggregatum* type structures], calcareous sponges (*Neuropora lusitanica* Termier, Termier & Ramalho) (Fig. 11b), crustaceans and echinoderm plates. Peloid dimension ranges from several microns to 1 mm. Subangular intraclasts have a microbial origin and they contain micropeloids and microbial structures (Fig. 11b). Porosity is completely lost by cementation (Fig. 11a–d).

Microfacies type 11 (Samples 2441–2444)—this rock is a carbonate microconglomerate with calcareous elements (Figs. 11e-h, 13). These clasts contain echinoderm plates and sponge spicules. They are mostly derived from peloidal boundstone microfacies types (Fig. 11e). Interparticle pores are well developed between quartz grains, peloids and echinoderm plates (Fig. 11f, h). The rock contains terrigenous material (quartz) (Fig. 11h).

XRD analysis

Facies analysis was performed on 30 samples. Out of the 30 samples considered for facies analyses, 13 were representative for XRD analysis. The results led to the separation of three distinct groups, based on their mineralogy (Fig. 14).

1. Pure limestones, consisting of calcite with very little quartz near the detection limit (the most intense peak at 26.64° barely visible)—9 samples (from microfacies types 4, 7–10 and 11);
2. Detrital limestones—3 samples, 2 of which are also dolomitic (2445B, microfacies type 1—quartz, pyrite; 2450, microfacies type 3—quartz, muscovite, kaolinite, pyrite (accessory); 2454b, microfacies type 6—quartz, feldspar, muscovite);
3. Silicified limestone (2453B, microfacies type 4).

Apparent density, mineral skeleton density, porosity

Moneasa zone

The apparent density ranges between 2.61 and 2.73 g/cm^3. Generally, the most common values range between 2.62 and 2.63 g/cm^3 with an average value of 2.65 g/cm^3 (Table 1).

The mineral skeleton density has a general value of 2.73 g/cm^3 with only two samples recording lower values (2.61 g/cm^3 and 2.62 g/cm^3) (Table 1). The total porosity varies from 0 to 5% (Table 1).

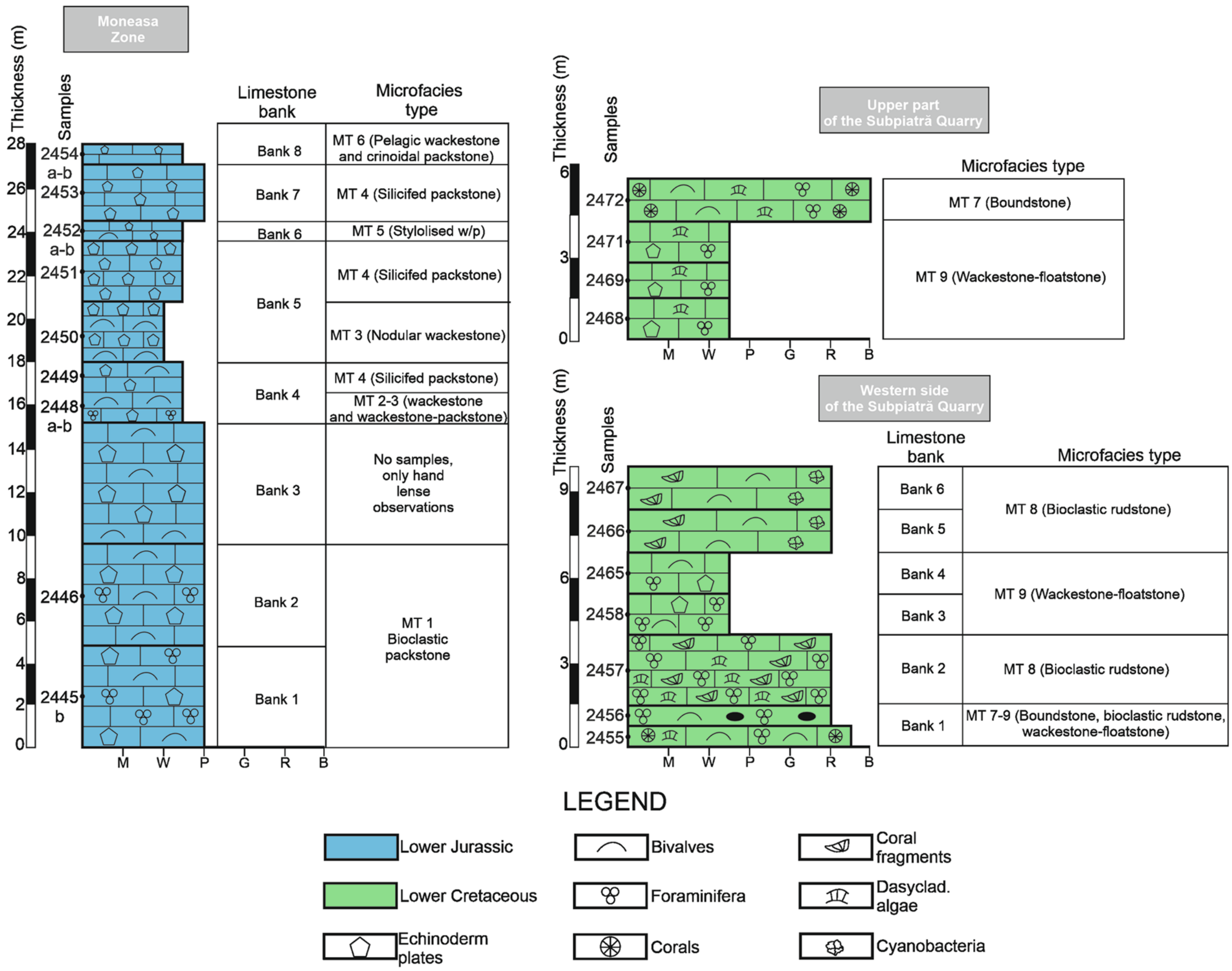

Fig. 12 Lithological columns and vertical facies distribution of the Lower Jurassic and Lower Cretaceous successions from the Moneasa and Subpiatră Zones

Subpiatră zone

The lowest value of the apparent density is 2.52 g/cm^3, while the highest value is 2.73 g/cm^3. The average value records 2.66 g/cm^3 (Table 1). The mineral skeleton density ranges from 2.60 to 2.75 g/cm^3. The average is 2.69 g/cm^3 (Table 1). The total porosity ranges between 0.4 and 5% (Table 1).

Sănduleşti zone

The apparent density of the samples ranges between 2.48 and 2.73 g/cm^3. Two groups of values characterise this property. The first group ranges between 2.48 and 2.50 g/cm^3, while the second group has the lowest value of 2.70 g/cm^3 and the highest value of 2.73 g/cm^3. The average is 2.62 g/cm^3 (Table 1). The mineral skeleton density ranges between 2.63 and 2.73 g/cm^3 (Table 1) and the total porosity varies from 0 to 7% (Table 1).

Uniaxial compressive strength

Moneasa zone

The lowest value has 7.56 MPa while the highest has 83.69 MPa. The vast majority of the values range between 44.81 and 57.86 MPa (Table 1).

Subpiatră zone

The uniaxial compressive strength ranges from 12.40 to 144.81 MPa. However, the most frequent values range between 51.76 and 76.98 MPa (Table 1).

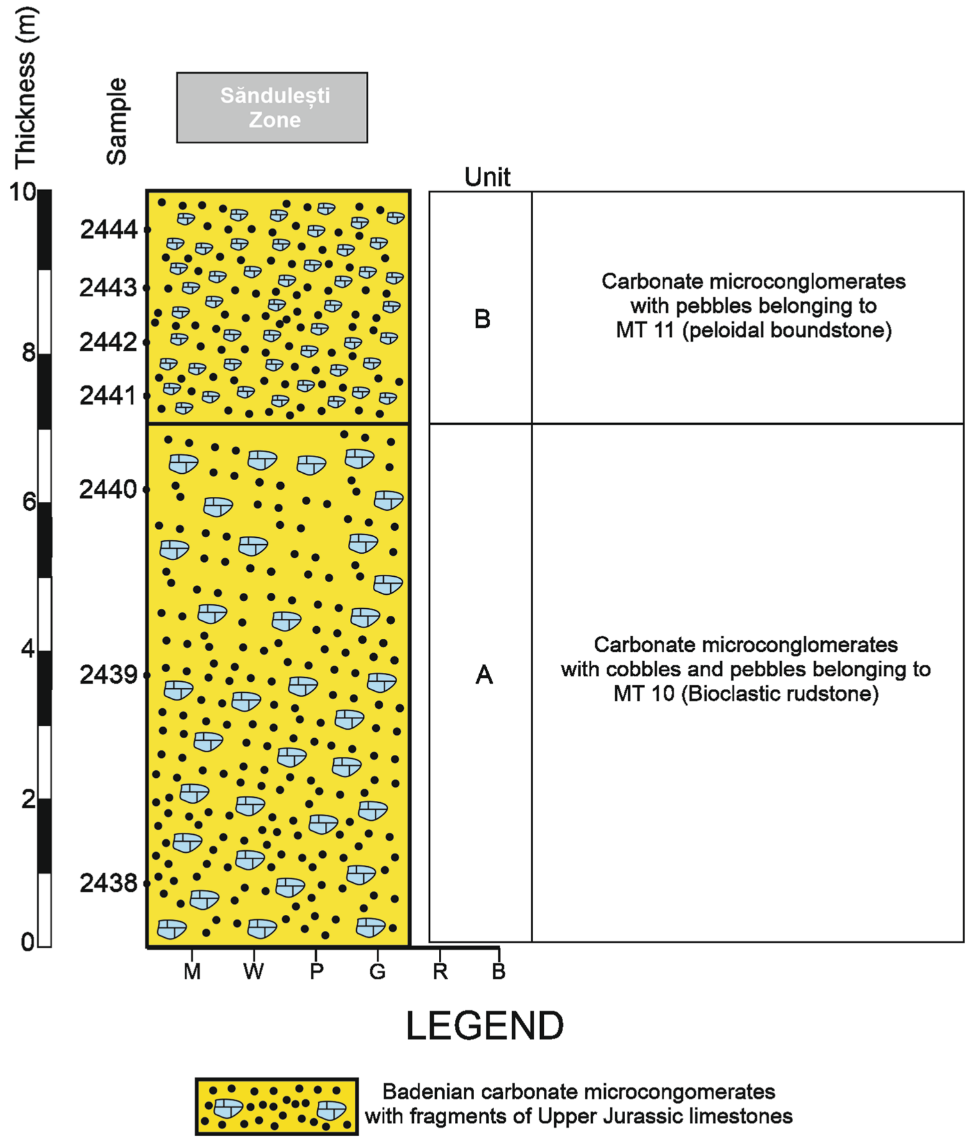

Fig. 13 Lithological column and vertical facies distribution of the Miocene (Badenian) succession from the Sândulești Zone

Sândulești zone

There are two major categories of values, the first one ranging from 30.11 to 43.36 MPa, and the second from 64.23 to 121.83 MPa (Table 1).

Discussions

Textural and chromatic homogeneity

Homogeneity is influenced by the textural and chromatic characteristics of the rocks (Carvalho and Lisboa 2018). The fracturing degree is indicated by the spatial arrangement of fractures and their scale of development (Carvalho and Lisboa 2018). In addition, rock uniformity (homogeneity of appearance dictated by colour and texture) represents a key aspect which has to be taken in consideration when evaluating ornamental rock potential (Arvantides and Heldal 2015). Microfacies types 1 and 4 are relatively homogeneous because they do not record major colour and textural changes. By contrast, microfacies types 2, 3 and 5 record important chromatic variations (the matrix is red and the clasts have a white to yellowish colour). Brecciation and stylolitisation strongly affects microfacies types 2–4 from the Moneasa Zone. The presence of stylolites filled with reddish material clearly influences the chromatic characteristics of these deposits. In some situations, the colour contrast between stylolite infill material and the general rock-mass may increase the aesthetic importance of ornamental rocks (Arzani 2011). Microfacies type 7 has important chromatic and textural variations, dictated by the colour difference between the corals and the internal sediment disposed between them. As a general rule, coarse bioclastic

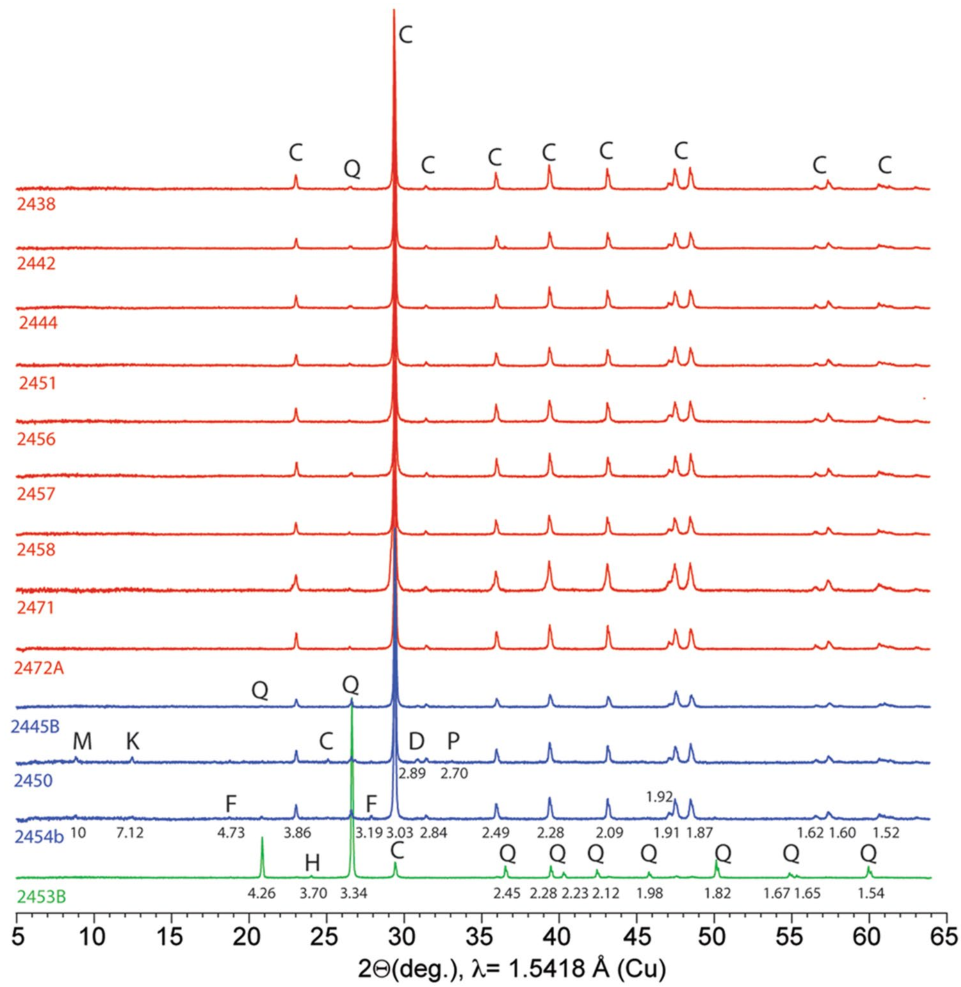

Fig. 14 XRD patterns of the 13 limestone samples, with d-spacings of the mineral reflections (in ångström), and intensity on the y-axis in arbitrary units; [pure limestones (red), detrital limestones (blue), silicified limestone (green). C—calcite, Q—quartz, D—dolomite, F—plagioclase feldspar, M—muscovite, H—hematite, P—pyrite]

limestones are less homogeneous in terms of texture and colour (Carvalho and Lisboa 2018). Colour variations may be indicated by the chromatic differences between grains and sparite or micrite. Microfacies types 8–9 are relatively homogeneous with only some slight colour changes. Such chromatic differences are generated by a slight contrast between the dark grey *Bacinella* type structures and the light grey micritic sediment that hosts them. Microfacies types 10–11 are relatively heterogeneous in terms of colour characteristics. Colour uniformity and homogeneity are very important when assessing the ornamental potential of a studied area (Papertzian and Farrow 1995). In terms of colour homogeneity, microfacies types 1, 4 and 8–9 are the most uniform. Microfacies types 5–11 (Subpiatră and Sănduleşti) contain rare fissures, with no significant fractures or other such features.

Relationship between physical–mechanical properties and petrography

Carbonate rock porosity directly influences permeability. Permeability in carbonate rocks is enhanced by the presence of fissures or fractures (Moore et al. 2011; Che et al. 2019). Total porosity ranges from 0 to 5% (Table 1). These limestones can be classified as rocks with negligible porosity (Levorsen 1967; Eysa et al. 2016). Only two samples (2442-1 and 2442-2) have a porosity of 5–7% (Table 1). Overall, these values characterise rocks with low porosity (Levorsen 1967).

The relationship between porosity and apparent density indicates that density decreases with increasing porosity (Fig. 15a) (Wang et al. 2009; Eysa et al. 2016; Salah et al. 2020). This tendency is confirmed by the existence of two major groups of values (A and B) (Fig. 15a), and the microfacies data can be partially correlated with these trends. For example, two lower density quartz rich samples from microfacies type 11 (2442-1 and 2442-2) show important microscopic porosity (Fig. 11h). In addition, group A

Table 1 Physical and mechanical properties of the studied samples

Studied area	Sample	Apparent density (g/cm^3)	Mineral skeleton density (g/cm^3)	Total porosity (%)	Uniaxial compressive strength (MPa)
Moneasa	2451	2.61	2.61	0	57.86
	2454 b-1	2.63	2.73	4	44.81
	2454 b-2	2.62	2.73	5	51.70
	2445 b-2	2.62	2.62	0	83.69
	2450	2.72	2.73	1	49.89
	2453 (B)	2.73	2.73	0	7.56
Subpiatră	2456 a-1	2.69	2.72	2	72.96
	2456 a-2	2.69	2.70	0.4	12.40
	2456 a-3	2.69	2.72	2	25.92
	2458-1	2.72	2.74	1	69.54
	2458-2	2.70	2.75	2	66.97
	2458-3	2.58	2.60	0.8	66.91
	2457	2.52	2.64	5	31.89
	2471-1	2.70	2.73	2	144.81
	2471-2	2.68	2.71	2	34.56
	2471-3	2.66	2.69	2	30.11
	2472 A-1	2.68	2.69	0.4	76.98
	2472 A-2	2.71	2.72	1	51.76
	2472 A-3	2.73	2.75	1	75.75
Sănduleşti	2438	2.73	2.73	0	121.83
	2438 a-1	2.70	2.71	1	64.23
	2438 a-2	2.70	2.63	1	75.59
	2442-1	2.50	2.64	6	30.11
	2442-2	2.48	2.66	7	43.36
	2444	2.63	2.66	2	37.91

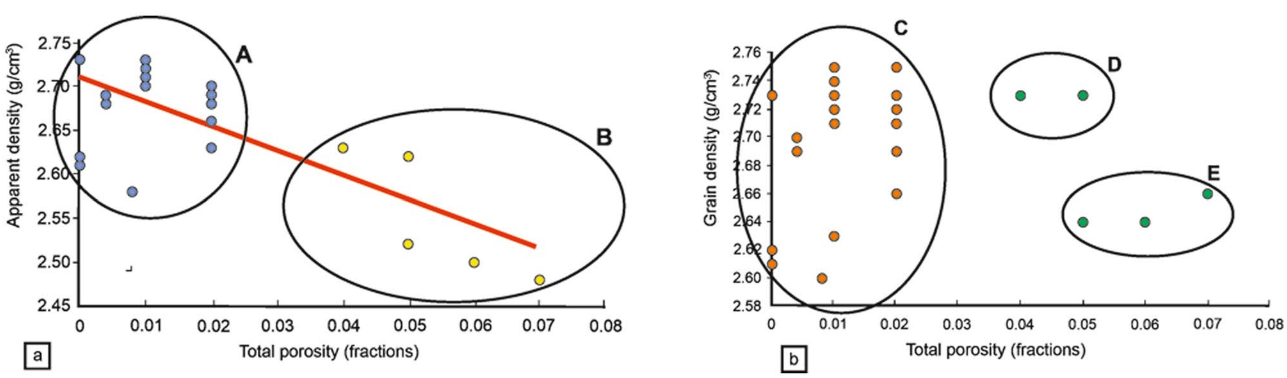

Fig. 15 Density vs total porosity cross-plots (**a**—apparent density vs total porosity. Density decreases with increasing porosity. Group A reunites samples with higher density and lower porosity while group B reunites samples with lower density and higher porosity; **b**—grain density vs total porosity. Group C contains samples with low porosity and high density. Group D contains samples with higher porosity and constant density. Group E contains samples that have the highest porosity)

(Fig. 15a) contains mainly samples with low porosity and higher density. This is confirmed by petrographic and microfacies data, since these samples are strongly compacted and all the porosities are lost by cementation.

The relationship between porosity and mineral skeleton density indicates three major trends. The first important group (C) has low porosity (0–2%) and a density that ranges from 2.60 to 2.75 g/cm^3 (Fig. 15b). The second group (D) has higher porosity (4–5%) and constant density (2.73 g/

cm^3) (Fig. 15b). The third group (E) has a porosity of 6–7% and a density of 2.64–2.66 g/cm^3 (Fig. 15b).

Group C corresponds to microfacies types 1–5 (Moneasa Zone) and 7–9 (Subpiatră Zone). These rocks are defined by negligible porosity and strong cementation. Microfacies types 1–5 contain numerous stylolites filled with clay material or organic matter. They correspond to sedimentary stylolites which are parallel or subparallel to the bedding planes (Ebner et al. 2010; Vandeginste and John 2013; Pleş et al. 2020). Group D corresponds to microfacies type 6 from Moneasa. Increased porosity and density can be associated with the presence of iron oxides as normally cementation by iron oxides may increase porosity and density (Eysa et al. 2016; Nabawy and Barakat 2017). In addition, brecciated limestones may record higher porosities (Smosna et al. 2005). The third group (E) contains mainly carbonate microconglomerates from microfacies type 11 (Săndulești Zone), their lower density (2.64–2.66 g/cm^3) correlating well with the increased porosity values.

Relationship between uniaxial compressive strength and microfacies types

The mechanical properties of rocks are influenced by their mineralogical composition, bioclast content, porosity and texture (Bell 1978; Shakoor and Bonelli 1991; Bell and Lindsay 1999; Naeem et al. 2014). Numerous previous studies were focussed on deciphering the relationship between UCS and rock petrography (Deere and Miller 1966; Williams et al. 1982; Irfan 1996; Prikryl 2001; Kilic and Teymen 2008). The highest UCS values are common for rocks that lack fractures, fissures or porosity (Fig. 16a). The nodular limestones from Moneasa break on contact areas between carbonate and clay material (Fig. 17e). The black limestone varieties (microfacies type 1) record higher UCS values (Fig. 17c, d) since fissures are absent (Fig. 17c). As a general rule, higher UCS values (Fig. 17b, d, h) characterise micritic homogeneous samples (Fig. 17a, c, g). By contrast, the lowest UCS values can be associated with grainy or brecciated samples (Fig. 17e, f).

Microfacies types 1, 3, 4, 5 and 6 have UCS values that range from 44.81 (sample 2454 b1) to 83.69 MPa (sample 2445 b2). Only one sample [2453 (B)] has lower values (Table 1). The Moneasa Limestone can be classified as a

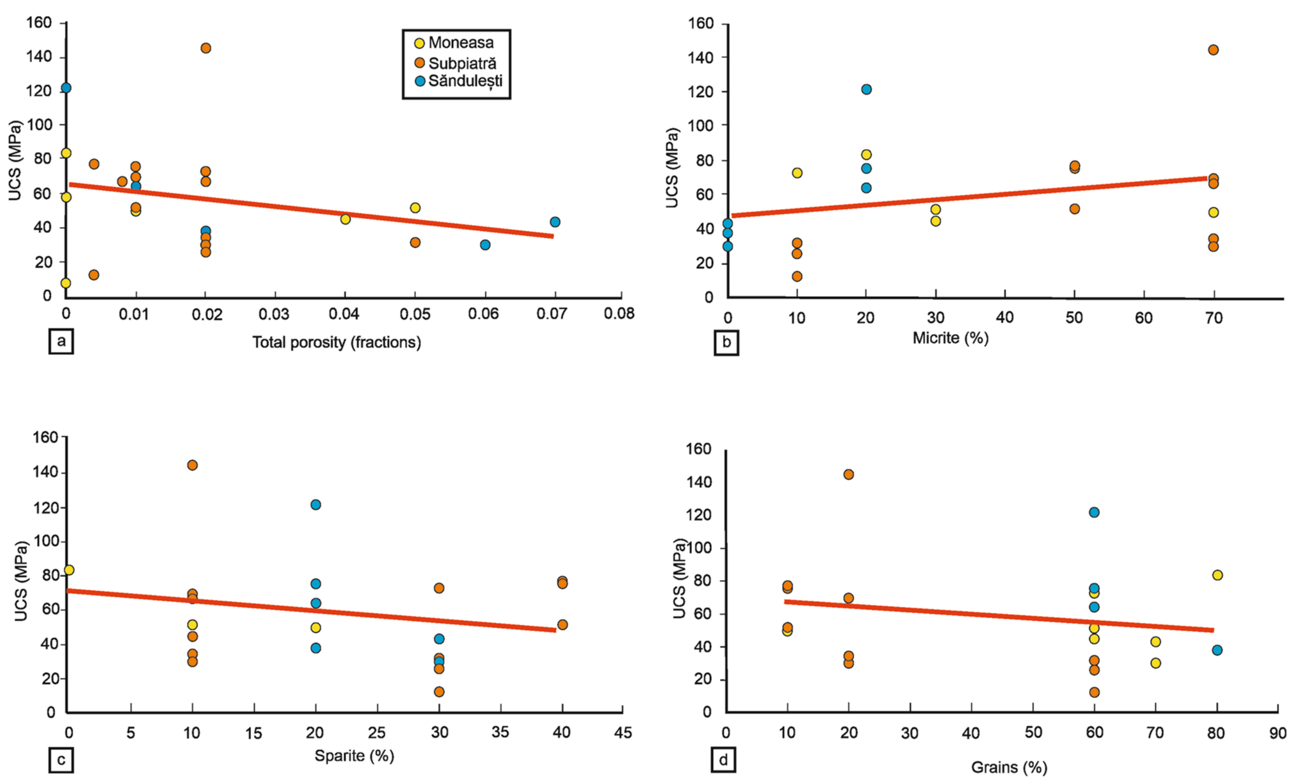

Fig. 16 Relationship between UCS and the petrographic characteristics of the studied deposits (**a**—relationship between UCS and porosity; **b**—relationship between UCS and micrite content; **c**—relationship between UCS and sparite content; **d**—relationship between UCS and grain content)

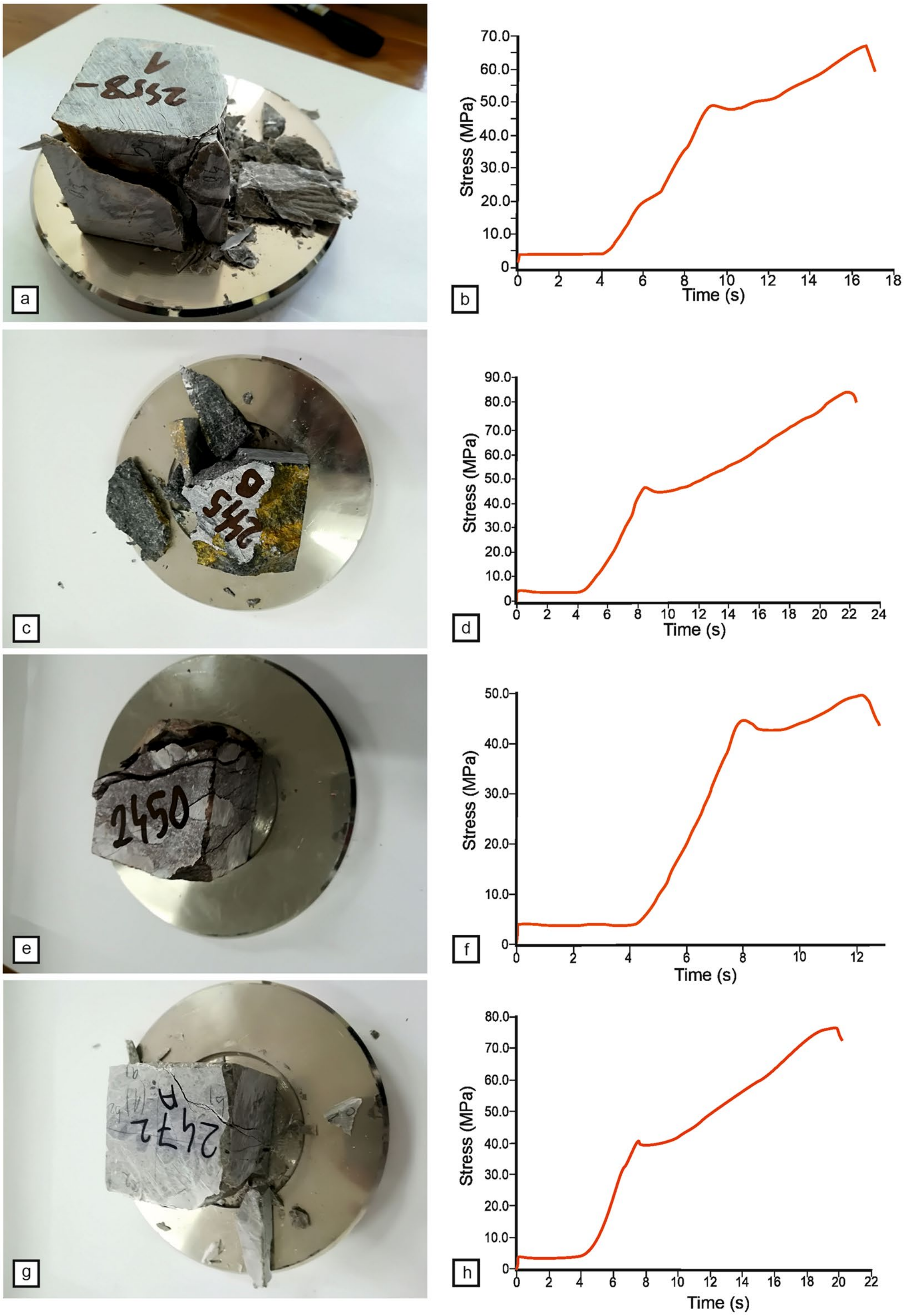

Fig. 17 Uniaxial compressive strength values for some of the studied limestones [**a**—oblique fractures in a bioclastic rudstone (microfacies type 9) from Subpiatră Quarry; **b**—uniaxial compressive strength values for sample 2458–1; **c**—black, homogeneous wackestone–packstone from microfacies type 1, Moneasa Quarry; **d**—uniaxial compressive strength values for sample 2445-B; **e**—nodular brecciated limestone from microfacies type 3, Moneasa Quarry; **f**—uniaxial compressive strength values for sample 2450; **g**—micritic limestone from microfacies type 7, Subpiatră Quarry; **h**—uniaxial compressive strength values for sample 2472 A-1] (scale: **a**, **c**, **e**, **g**—10 mm)

moderately tough to tough rock (Deere and Miller 1966; Beniawski 1984). According to the International Society of Rock Mechanics (1981), these limestones have a medium resistance. There is a clear relationship between UCS and porosity (Fig. 16a). Sample 2445 b2 from microfacies type 1 has zero porosity (Fig. 16a) and high UCS values (83.69 MPa). Sample 2451 from microfacies type 4 records an UCS value of 57.86 MPa, for zero porosity (Fig. 16a). On the contrary, samples from microfacies type 6 (2454 b1, 2454 b2) record lower UCS values (44.81 and 51.7 MPa) for slightly higher porosities (4–5%) (Fig. 16a). Such lower UCS values can be explained by this slight increase in porosity. In fact, even small-scale porosity variations can determine a decrease in UCS values (Naeem et al. 2014).

The average UCS values of the Subpiatră Limestone range from 37.09 to 69.82 MPa.

Sample 2456 has an average UCS value of 37.09 MPa (Table 1). This value marks the cutoff between rocks with weak and medium resistance (International Society of Rock Mechanics 1981). According to other classifications (Beniawski 1973) it can be labelled as a weak rock.

The average UCS value for sample 2458 is 67.80 MPa. Sample 2471 records an average UCS of 69.82 MPa while sample 2472 has an average of 68.16 MPa. They can be defined as very tough to tough rocks (Beniawski 1984). According to other classifications (Coates 1964), these samples are situated at the limit between weak and tough rocks. Finally, they can be classified as moderately resistant rocks (Deere and Miller 1966). The samples with low porosity (1–2%) record higher UCS values (up to 144 MPa). In the same manner, an increase in porosity (5%) can be associated with lower UCS values (31.89 MPa) (Fig. 16a). In addition, an increase in micrite content (50 to 70%) is associated with higher UCS values (Fig. 16b). By contrast, less micrite and more sparite corresponds to lower UCS values (Fig. 16c). Samples with abundant grains (60%) may record lower UCS values than samples with less grain percentages (10–20%) (Fig. 16d). Similar correlation patterns were established for carbonate rocks by Akram et al. (2017).

The carbonate samples from Sândulești (2438 and 2438 a) have an average UCS value of 87.21 MPa (Table 1). They can be classified as moderately to extremely tough rocks (Deere and Miller 1966; International Society of Rock Mechanics 1981; Beniawski 1984). As a general rule, the samples with low porosity (2472 A-1, 2472 A-2, 2472 A-3) record higher UCS values (Table 1) (Fig. 16a). In general, the UCS values increase as porosity decreases (Naeem et al. 2014; Akram et al. 2017).

The other samples from Sândulești (2442 and 2444, microfacies type 11) record average UCS values of 36.73 MPa and 37.91 MPa. These rocks can be classified as weakly resistant (Coates 1964; Deere and Miller 1966 or Beniawski 1984). Samples with low porosity (2438 a-1, 2438 a-2) record the highest UCS values (Table 1) (Fig. 16a). A high percentage of grains (80%) can be associated with lower UCS values. By contrast, a decrease in grain percentage (60%) may correspond to higher UCS values (Fig. 16d). This model corresponds with similar trends obtained by Akram et al. (2017) for limestones and other carbonate rocks.

Potential ornamental limestone areas

Ornamental limestone quarrying areas can be divided in four important categories (Carvalho and Lisboa 2018): (1) consolidated exploitation areas-quarrying is continuous and a re-evaluation of the existing resources is necessary; (2) complementary exploitation areas—these areas contain exploitable resources but they are strongly susceptible to reserve depletion; (3) potential areas—the existing data suggest that these zones contain enough reserves to become consolidated exploitation areas; (4) rehabilitation areas—in these zones, ornamental rock quarrying is not possible anymore and environmental rehabilitation is necessary. The existing data indicate that the Moneasa and Subpiatră Limestones could be used for interior and exterior cladding.

Limestones for exterior and interior cladding have to be analysed according to the EN 1469 standard. First, the dimension criteria have to be established. Second, their colour, texture, homogeneity and fracturing degree has to be determined. Third, petrographic analysis is necessary. Finally, physical and mechanical tests have to be performed to determine various properties (apparent density, total porosity, uniaxial compressive strength, flexural resistance, etc.). According to Amaral et al. (2015), additional tests such as durability are necessary. This study follows the methods described in the SR EN 1469 standard.

Moneasa zone

These limestones were used extensively for inner cladding works (Pârvu et al. 1977). The term “Moneasa Marble” has a strict commercial meaning even if it was used intensively in the past to characterise these limestones. Carbonate rocks are usually classified as marbles in the ornamental limestone industry (Amaral et al. 2015). However, all the petrographic characteristics suggest that these rocks are limestones. Therefore, this commercial denomination takes into account only the effort necessary to polish the rock surface (Amaral et al. 2015). These limestones were used extensively for interior and exterior cladding works, pavements and stepways in the former Austro-Hungarian Empire and in Romania (Fig. 18a–h). Exterior cladding usage can pose some difficulties since these limestones contain abundant stylolites and areas with detrital material and iron oxides. Thus, they are more sensitive to weathering

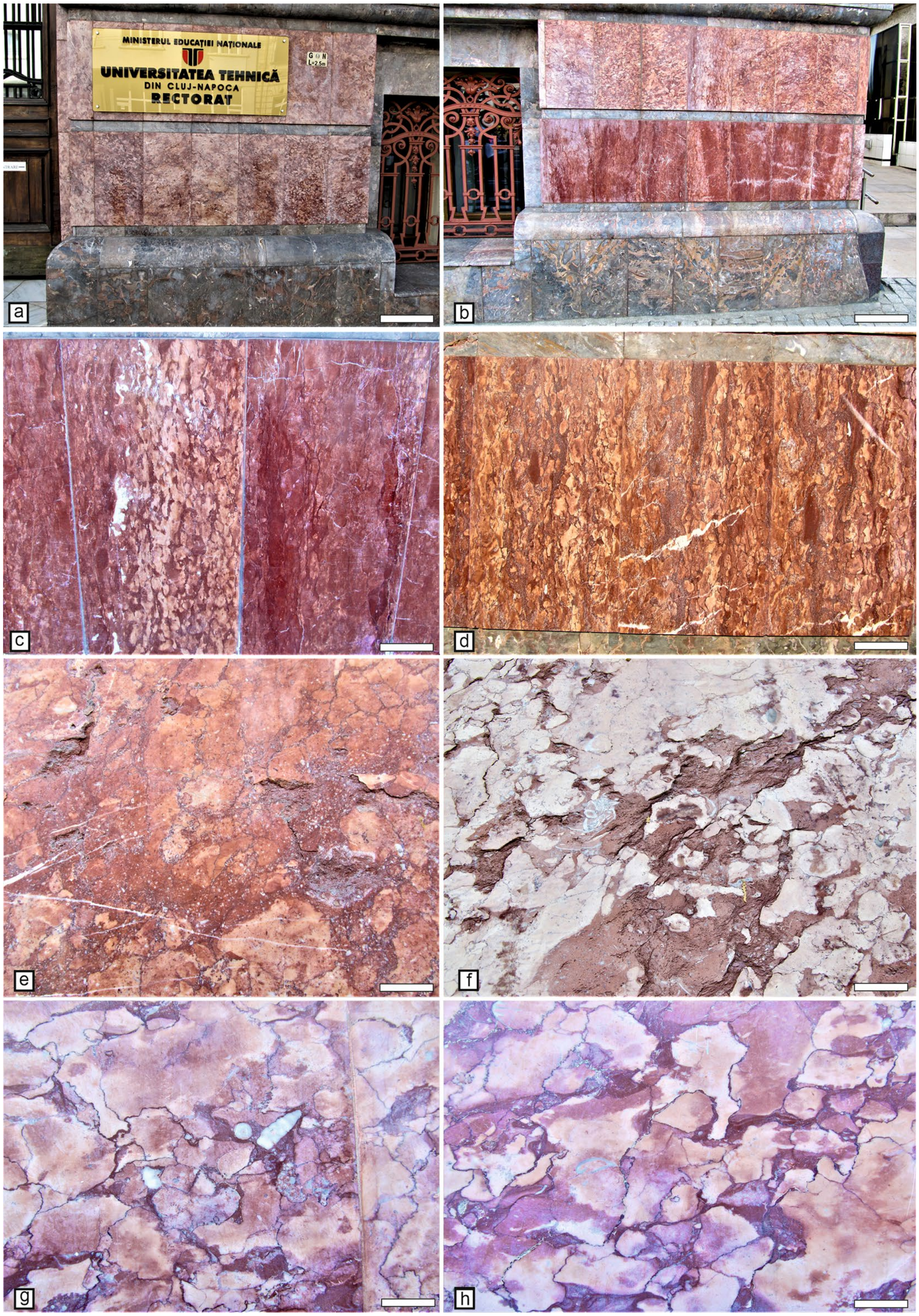

Fig. 18 Moneasa Limestone used for exterior cladding on various buildings from Cluj Napoca (**a**, **b**—centimetre-to-decimetre-scale cladding tiles consisting of nodular, brecciated, red to yellowish limestones; **c**—interbeddings of yellowish-brown and red nodular limestones. Sparite filled voids develop at the contact between these limestone varieties; **d**—alternating nodular and crinoidal limestones. Numerous stylolites are present and oblique fractures are filled with sparite; **e**—contact between crinoidal packstone and nodular limestone. Cracks and fissures start to develop in areas filled with clay material and iron oxides; **f**—nodular limestone with iron oxides and clay material disposed between the nodules. These areas are more sensitive to weathering and erosion; **g**, **h**—stylolised nodular limestone with belemnites and other pelagic organisms) (**a**–**e**—Technical University of Cluj Napoca; **f**–**h**—Babeş-Bolyai University, Department of Geology) (scale: **a**, **b**—40 cm; **c**, **e**—20 cm; **f**–**h**—3 cm)

processes (Fig. 18e, f). The dimension criteria is met in this case because the average carbonate bank thickness from the Moneasa Quarry exceeds 1 m. In addition, the standard reference sample for interior cladding does not have to exceed 0.25 square metres (Amaral et al. 2015; SR EN 1469 standard). Microfacies types 2, 3 and 5 present low textural and chromatic homogeneity. These limestones could be defined as rocks with low porosity and medium fracturing degree (Fourmaintraux 1976). According to the American standard ASTM-C568-C568M, dimension limestones require a minimum UCS value of 55 Mpa and a minimum density of 2.56 g/cm^3 (ASTM 2006). Only microfacies type 1 (sample 2445-b2) and 4 (sample 2451) (Table 1) exceed this threshold. The samples from microfacies type 1 are texturally and chromatically homogeneous and their black colour could recommend them for funeral plaques or inner fireplaces. However, additional analyses are necessary to confirm this (e.g. frost resistance, flexural strength, and thermal expansion coefficient) (Amaral et al. 2015).

The reserves are abundant and the exploitation could continue in the future, for a couple of years. Until 1990, the entire area was active; however, at the moment, the quarry is closed due to administrative disputes.

Subpiatră zone

The Subpiatră Limestone is quarried for cement production by the LaFarge Holcim company. Samples from microfacies types 7–9 could be used for interior and exterior cladding. The dimension criteria are met (SR EN 1469 standard) because the studied limestones are stratified in decimetre-to-metre-thick banks, with an average thickness of 1 m. The UCS values (Table 1) indicate that samples 2458, 2471 and 2472 (microfacies types 7 and 9) are the most resistant. Their UCS exceeds 55 MPa, in agreement with the minimum value requested by the ASTM-C568-C568M (ASTM 2006). Boundstone and wackestone facies are the most suitable for ornamental limestone production while the rudstone facies are less suitable because their UCS values do not meet the minimum threshold requested by the American standard ASTM-C568-C568M (ASTM 2006). The Subpiatră Limestone can be classified as a slightly fissured rock with very low porosity (Fourmaintraux 1976). Microfacies type 9 contains the most homogeneous samples. Their low porosity and lack of fracturing indicates strong resistance to weathering and they may be used for exterior cladding, but additional tests (flexural resistance, durability) (Amaral et al. 2015) should be performed to eliminate any uncertainties. Their physical and mechanical properties are similar with those of other Mesozoic (Jurassic and Cretaceous) analogue deposits from other areas of the Southern Carpathians (Pârvu et al. 1977). These values recommend them for ornamental limestone quarrying, even if they are extensively quarried for cement production at the moment. The Subpiatră Zone qualifies for a potential ornamental limestone area (sensu Carvalho and Lisboa 2018).

Săndulești zone

The existing microfacies types have different characteristics. Microfacies type 10 contains well-rounded, Upper Jurassic pebbles. Their physical and mechanical properties are the same with those of adjacent limestones exploited at Tureni or in the Săndulești Limestone Quarry (Pârvu et al. 1977). In addition, this facies type is widespread in other parts of the Romanian Carpathians (Piatra Craiului-Dâmbovicioara, Postăvaru and Buila-Vânturarița Massifs) (Bucur et al. 2010; Pleș 2016; Mircescu et al. 2019; Șerban et al. 2020). Some pebbles from this facies record UCS values of 70 MPa (Samples 2438 a-1 and 2438 a-2, Table 1). Pârvu et al. (1977) have reported slightly higher UCS values for the autochthonous Upper Jurassic carbonates of the Săndulești Zone. The difference is given by the allochthonous character of the pebbles. They were transported on short distances, as reworked material in the general mass of the Badenian carbonate microconglomerates. As a consequence, they have lost some of their strength. These UCS values are similar with data reported by Pârvu et al. (1977) from the Upper Jurassic deposits of the Postăvaru Massif (Temelia Quarry) or from Buila Vînturarița (Arnota Quarry). The carbonate pebbles from microfacies type 10 meet all the requirements for ornamental and dimension stone (American Standard ASTM-C568-C568M) (ASTM 2006), but the greatest uncertainties are linked with the small volume of reserves and reduced outcrop dimensions. Microfacies type 11 (samples 2442-1, 2442-2 and 2444) contains samples with low UCS values and high porosity (6–7%). Such terrigenous Badenian carbonate microconglomerates were used by the Romans, during the third century AD as raw materials (wrought blocks) for the Potaissa camp (Bărbulescu 1994). They were quarried from the Piatra Tăiată archaeological site, situated in the vicinity of the Roman Spring (Bărbulescu 1994). However, the physical and mechanical properties question their suitability as ornamental rocks.

Conclusions

1. This study analyses the ornamental characteristics of carbonate deposits from three distinct locations belonging to three different tectonic units of the Apuseni Mountains. Microfacies analysis was correlated with physical and mechanical rock properties to define several types of ornamental limestones.
2. The physical–mechanical properties correlate well with microfacies analysis. Generally, limestones with low

porosity have the highest UCS values. In addition, the micritic and bioconstructed facies are the most suitable for ornamental stone quarrying. By contrast, the brecciated and fractured facies are not suitable for such activities.
3. This study confirms that the carbonate rocks from Moneasa can be used for interior cladding. A potential ornamental limestone area is defined in the Subpiatră Zone. These rocks may be used in the future for interior and exterior cladding. By contrast, the carbonate deposits from Săndulești show important uncertainties concerning their ornamental potential.

Acknowledgements This work received financial support through the project Entrepreneurship for Innovation Through Doctoral and Postdoctoral Research (POCU/360/6/13/123886) co-financed by the European Social Fund through the Operational Program for Human Capital 2014–2020. It is also a contribution to a Postdoctoral Research Programme (Babeș-Bolyai University of Cluj Napoca) titled "Practical applications for the usage of various Mesozoic limestones from the Romanian Carpathians for ornamental and decorative purposes". The first author (CVM) acknowledges partial funding from a grant of the Ministry of Research, Innovation and Digitization, CNCS/CCCDI-UEFISCDI, project number PN-III-P1-1.1-PD-2019-0456 within PNCDI III. The authors thank Victor Mircescu and Alin Oprișa for their fieldwork assistance and the LaFarge Holcim company for granting access in the Subpiatră Quarry. The anonymous reviewers are thanked for their valuable comments that helped improve a previous version of the manuscript.

Funding This work received financial support through the project Entrepreneurship for Innovation Through Doctoral and Postdoctoral Research (POCU/360/6/13/123886) co-financed by the European Social Fund through the Operational Program for Human Capital 2014–2020. The first author (CVM) acknowledges partial funding from a grant of the Ministry of Research, Innovation and Digitization, CNCS/CCCDI-UEFISCDI, project number PN-III-P1-1.1-PD-2019-0456 within PNCDI III.

Data availability The datasets generated during and/or analysed during the current study are available from the corresponding author on reasonable request.

Declarations

Conflict of interest The authors have no conflicts of interest to declare that are relevant to the content of this article.

References

Akram MS, Farooq S, Naeem M, Gazi S (2017) Prediction of mechanical behaviour from mineralogical composition of Sakesar limestone, Central Salt range, Pakistan. Bull Eng Geol Environ. https://doi.org/10.1007/s10064-016-1002-3

Amaral PM, Ferandes JC, Pires V, Rosa LG (2015) Ornamental stones. In: Goncalves MC, Margarido F (eds) Materials for construction and civil engineering. Springer, Cham. https://doi.org/10.1007/978-3-319-08236-3_9

Arvantides L, Heldal T (2015) Draft report: state of the art: ornamental stone quarrying in Europe, 57 p, OSNET Project. https://www.ngu.no/FileArchive/91/OSNET3.pdf

Arzani N (2011) Stylolite networks in dolomitized limestones and their control on polished decorative stones: a case study from Upper Cretaceous Khur quarries, central Iran. Jgeope 1(2):25–37

ASTM. Annual Book of ASTM standards, section 4: construction, volume 04.07 Building seals and sealants; fire standards; dimension stone (2006) American Society for Testing and Material. Philadelphia, USA

Balintoni I (1997) The geotectonics of the metamorphic terrains from Romania (in Romanian). Editura Carpatica, Cluj Napoca

Balintoni I, Puște A (2002) New lithostratigraphic and structural aspects in the southern part of the Bihor Massif (Apuseni Mountains). Studia UBB Geol 67:13–18

Balintoni I, Balica C, Cliveți M, Li-Qiu L, Horst PH, Chen F, Schuller V (2009) The emplacement age of the Muntele Mare Variscan granite (Apuseni Mountains, Romania). Geol Carp 60(6):495–504

Bărbulescu M (1994) Potaissa. Monographic study (in Romanian). Dissertationes Musei Potaissensis, Turda

Bell FG (1978) Physical and mechanical properties of the Fell sandstones. Northumberl Engl Eng Geol 12(1):1–29

Bell FG, Lindsay P (1999) The petrographic and geo-mechanical properties of some sandstone from the Newspaper Member of the Natal Group near Durban, South Africa. Eng Geol 53:57–81

Beniawski ZT (1973) Engineering Classifications of Jointed Rock Masses. Transact South Afr Institut Civil Eng 15(12):335–344

Beniawski ZT (1984) Rock mechanics design in mining and tunneling. AA Balkema Publishers, Rotterdam

Bleahu M, Borcoș M, Savu H (1967) Geological Map of Romania, sheet L-34-XVII Brad, scale 1:200 000 (in Romanian). Geological Institute, Bucharest

Bleahu M, Lupu M, Patrulius D, Bordea S, Ștefan A, Panin Ș (1981) The structure of the Apuseni Mountains. Inst Geol Geophys, 12th Congress of the Carpatho-Balkanian Association, Guidebook nr. 23, Excursion B3, 103 p

Bucur II (2000) Lower cretaceous dasyclad algae from the Pădurea Craiului Massif (Northern Apuseni Mountains, Romania). Acta Pal Rom 2:53–72

Bucur II, Săsăran E, Balica C, Beleș D, Bruchental C, Chendeș C, Chendeș O, Hosu A, Lazăr DF, Lăpădat A, Marian AV, Mircescu C, Turi V, Ungureanu R (2010) Mesozoic carbonate deposits from some areas of the Romanian Carpathians-case studies. Cluj University Press, Cluj Napoca

Bucur II, Saint-Martin JP, Filipescu S, Săsăran E, Pleș G (2011) On the presence of green algae (Dasycladales, Bryopsidales) in the Middle Miocene deposits from Podeni (western border of the Transylvanian Basin, Romania). Acta Pal Rom 7:69–75

Calvo JP, Reguiero M (2010) Carbonate rocks in the Mediterranean region—from classical to innovative uses of building stone. In: Smith BJ, Gomez-Heras M, Viles A, Cassar J (eds) Limestone in the built environment: present-day challenges for the preservation of the past, 331. Geological Society of London, London, pp 27–35

Carvalho JMF (1997) Calcários Ornamentais e Industriais da Área de Pé da Pedreira (Maciço Calcário Estremenho) - Carta de Aptidão. Estudos, Notas e Trabalhos Do IGM 39:71–89

Carvalho JMF, Lisboa JV (2018) Ornamental stone potential areas for land use planning: a case study in a limestone massif from Portugal. Env Earth Sci 77:206

Carvalho JMF, Lisboa JV, Moura AC, Carvalho C, Sousa LMO, Leite MM (2013) Evaluation of the Portuguese ornamental stone resources. Key Eng Mat 548:3–9

Catullo TA (1853) Intorno ad una nuova classificazione delle calcarie rosse ammonitiche delle Alpi Venete. Mem Inst Ven Sci 5:187–241

Che Z, Tan X, Deng J, Jin M (2019) The characteristics and controlling factors of facies-controlled coastal eogenetic karst: insights from the Fourth Member of Neoproterozoic Dengying Formation, Central Sichuan Basin, China. Carb Ev 34:1771–1783

Coates DF (1964) Classification of rocks for rock mechanics. Int J Rock Mech Min Sci 1:412–429

Cociuba I (2000) Upper Jurassic-Lower Cretaceous deposits in the south-western part of Pădurea Craiului. Formal Lithostratigraphic Units Studia UBB Geol 45(2):33–61

Deere DU, Miller RP (1966) Engineering classification and index properties of intact rock. AFNL-TR-65-116. AF Weapons Laboratory, Kirtland

De Zigno A (1850) Coup d'oeil sur les terrains stratifiés des Alpes Vénétiennes. Naturw Abh 4:1–16

Dunham RJ (1962) Classification of sedimentary rocks according to depositional structure. In: Ham WE (ed) Memoir 1st Edition. American Association of Petroleum Geologists, 1st Edition, Tulsa, Oklahoma, pp 235–239

Ebner M, Piazolo S, Renard F, Koehn D (2010) Stylolite interfaces and surrounding matrix material: nature and role of heterogeneities in roughness and microstructural development. J Str Geol 32:1070–1084

Eysa EA, Ramadan FS, El Nady MM, Said NM (2016) Reservoir characterization using porosity-permeability relations and statistical analysis: a case study from North-Western Desert. Egypt Arab J Geosci 9:403

Filipescu S, Gârbacea R (1997) Lower Badenian sea level drop on the western border of the Transylvanian Basin: foraminiferal paleobathymetry and stratigraphy. Geol Carp 48(5):325–334

Fourmaintraux D (1976) Characterisation of rocks; Laboratory tests. In: Panet M et al (eds) La Meccanique des roches appliquee aux ouvrages du genie civil. Ecole Nationale des Ponts et Chaussees, Paris

Giușcă D, Bleahu M, Lupu M, Borcoș M, Lupu D, Bițoianu C (1968) Geological map of Romania, sheet L-34-XI, Șimleul Silvaniei scale 1:200,000 (in Romanian). Geological Institute, Bucharest

Hoeck V, Ionescu C, Balintoni I, Koller F (2009) The Eastern Carpathians, ophiolites, (Romania): Remnants of a Triassic ocean. Lithos 108:151–171

Ianovici V, Borcoș M, Bleahu M, Patrulius D, Lupu M, Dimitrescu R, Savu H (1976) Geology of the Apuseni Mountains (in Romanian). Editura Academiei Republicii Socialiste România, București

International Society for Rock Mechanics (ISRM) (1981) Rock characterization, testing and monitoring—ISRM suggested methods. Pergamon Press, Oxford

Irfan TY (1996) Mineralogy fabric properties and classification of weathered granites in Hong Kong. Q J Eng Geol Hydrogeol 29:5–35

Kilic A, Teymen A (2008) Determination of mechanical properties of rocks using simple methods. Bull Eng Geol Environ 67:237–244

Kounov A, Schmid SM (2012) Fission-track constraints on the thermal and tectonic evolution of the Apuseni Mountains (Romania). Int J Earth Sci 102:207–233

Levorsen AI (1967) Geology of petroleum. WH Freeman and Company, San Francisco

Mircescu CV, Bucur II, Săsăran E, Pleș G, Ungureanu R, Oprișa A (2019) Facies avolution of the Jurassic-Cretaceous transition in the Eastern Getic Carbonate Platform, Romania: Integration of sequence stratigraphy, biostratigraphy and isotope stratigraphy. Cret Res 99:71–95

Misik M (1964) Lithofazielles Studium des Lias der Großen Fatra und des westlichen Teils der Niederen Tatra. Sbornik Geol Vied. Zapadne Karpaty, Rad ZK, Zväzok 1:9–92

Moore PJ, Martin JB, Screaton EJ, Neuhoff PS (2011) Conduit enlargement in an eogenetic karst aquifer. J Hydrol 393:143–155

Murray RC, Pray LC (1965) Dolomitization and limestone diagenesis—an introduction. In: Pray LC, Murray C (eds) Dolomitization and limestone diagenesis. SEPM Special Publications 13:1–2

Nabawy B, Barakat M (2017) Formation evaluation using conventional and special core analyses: Belayim formation as a case study, Golf of Suez. Egypt Ar J Geosci 10:25

Naeem M, Khalid P, Sanaullah M, Din ZU (2014) Physiomechanical and aggregate properties of limestones from Pakistan. Acta Geod Geophys 49:369–380

Papertzian C, Farrow D (1995) Dimension stone: a guide to prospecting and developing, open fle report. Ontario Geological Survey, Sudbury

Pârvu G, Mocanu G, Hibomvschi C, Grecescu A (1977) Utile rocks from Romania (in Romanian). Editura Tehnică, București

Pinter F, Szakmany G, Demeny A, Toth M (2014) The provenance of, red marble, monuments from the 12th–18th centuries. Eur J Mineral 16:619–629

Pleș G (2016) Upper Jurassic-lower cretaceous limestones from Buila-Vânturarița Massif in Romanian. Cluj University Press, Cluj Napoca

Pleș G, Kövecsi S, Bindiu Haitonic R, Silye L (2020) Microfacies analysis and diagenetic features of the Eocene nummulitic accumulations from northwestern Transylvanian Basin. Facies 66(3):20

Prikryl R (2001) Some micro structural aspects of strength variation in rocks. Rock Mech Min Sci 38:671–682

Robertson AHF, Mountrakis D (2006) Tectonic development of the eastern Mediterranean region. Geol Soc London Spec Publ 260(1):1–9

Romanian Standard STAS 6200/13-80 (1974) Natural stones for construction (in Romanian). Romanian Institute of Standardisation, Bucharest

Rusu A, Lupu M, Nicolae I, Pană D, Popescu G, Szasz L, Tatu D (2018) Geological Map of Romania, sheet L-34-60-A, Tureni, scale 1:50 000 (in Romanian). Geological Institute, Bucharest

Salah MK, Alqudah M, David C (2020) Petrophysical and acoustic assessment of carbonate rocks, Zahle area, central Lebanon. Bull Eng Geol Env 79:5455–5475

Săndulescu M (1984) Geotectonics of Romania (in Romanian). Editura Tehnică, București

Săndulescu M, Kräutner HG, Balintoni I, Russo-Săndulescu M, Micu M (1981) The Structure of the East-Carpathians (Moldavia-Maramureș area). Inst Geol Geophys, 12th Congress of the Carpatho-Balkanian Association, Guidebook no. 21, Excursion B1, 92 p

Săsăran E (2006) Upper Jurassic-Lower Cretaceous limestones from the Trascău Mountains (in Romanian). Cluj University Press, Cluj Napoca

Schmid SM, Bernoulli D, Fügenschuch B, Mațenco L, Schefer S, Schuster R, Tischler M, Ustaszewski K (2008) The Alpine-Carpathian-Dinaridic orogenic system: correlation and evolution of tectonic units. Swiss J Geo 101(1):139–183

Șerban S, Mircescu CV, Ungureanu R, Bucur II (2020) Carbonate clasts from Cretaceous conglomerate deposits of the Postăvaru Massif (Southern Carpathians, Romania). Depositional environments and biostratigraphic remarks. Acta Pal Rom 17(1):27–39

Shakoor A, Bonelli RE (1991) Relationship between petrographic characteristics, engineering index properties and mechanical properties of selected sandstone. Bull as Eng Geol 28:55–71

Siegiesmund S, Grimm WD, Durast H, Ruedrich J (2010) Limestones in Germany used as building stones: an overview. In: Smith BJ,

Gomez-Heras M, Viles A, Cassar J (eds) Limestone in the built environment: present-day challenges for the preservation of the past, vol 33. Geological Society of London, London, pp 137–59
Smosna R, Bruner KR, Riley RA (2005) Paleokarst and reservoir porosity in the Ordovician Beekmantown dolomite of the central appalachian basin. Carb Ev 20:50–63
Standard SR EN 1097-6 (2002) Test for mechanical and physical properties of aggregates. Part 6: determination of particle density and water absorption. European Committee for Standardization
Standard SR EN 1469 (2015) Natural stone products. Slabs for cladding. Requirements. European Committee for Standardization
Tudoran A (1997) Biostratigraphical and palaeoenvironmental significance of Jurassic microfossils from Romania. PhD Thesis, Louisiana State University and Agricultural & Mechanical College
Vandeginste V, John CM (2013) Diagenetic implications of stylolitization in Pelagic Carbonates, Canterbury Basin, Offshore, New Zealand. J Sed Res 83(3):226–240
Wang JH, Hung JH, Dong JJ (2009) Seismic velocities, density, porosity, and permeability measured at a deep hole penetrating the Chelungpu fault in central Taiwan. J Asian Earth Sci 36:135–145
Williams H, Turner FJ, Gilbert CM (1982) Petrography: an Introduction to the Study of Rocks in Thin Section. WH Freeman and Company, San Franscisco